

Power Corrections in Charmless Nonleptonic $B \rightarrow D$ decays: Annihilation is Factorizable and Real

Christian M. Ameshen,¹ Zoltan Ligeti,^{2,1} Ira Z. Rothstein,³ and Iain W. Stewart¹

¹Center for Theoretical Physics, Laboratory for Nuclear Science, Massachusetts
 Institute of Technology, Cambridge, MA 02139

²Ernest Orlando Lawrence Berkeley National Laboratory, University of California,
 Berkeley, CA 94720

³Department of Physics, Carnegie Mellon University, Pittsburgh, PA 15213

Abstract

We classify $\mathcal{O}_{\text{CD}} = m_b$ power corrections to nonleptonic $B \rightarrow M_1 M_2$ decays, where $M_{1,2}$ are charmless non-isosinglet mesons. Using recent developments in soft-collinear effective theory, we prove that the leading contributions to annihilation amplitudes of order $\mathcal{O}_s(m_b) \mathcal{O}_{\text{CD}} = m_b$ are real and are determined by distribution functions that already occur in the lowest order $B \rightarrow M_1 M_2$ factorization theorem. A complex nonperturbative parameter from annihilation first appears at $\mathcal{O}_s(\overline{m_b}) \mathcal{O}_{\text{CD}} = m_b$. "Chirally enhanced" contributions are also factorizable and real at lowest order. Thus, incalculable strong phases are suppressed in annihilation amplitudes, unless the $\mathcal{O}_s(\overline{m_b})$ expansion breaks down. Modeling the distribution functions, we find that (11–9)% and (15–11)% of the absolute values of the measured $B^0 \rightarrow K^+ K^-$ and $B \rightarrow K^+ K^0$ penguin amplitudes come from annihilation. This is consistent with the expected size of power corrections.

I. INTRODUCTION

Nonleptonic charmless B decays are important probes of the standard model. They are sensitive to the CP violating phase (or) via the interference of tree and penguin contributions, and to possible new physics that could modify the penguin amplitudes. They also provide a powerful laboratory to study strong interactions, the understanding of which is crucial if one is to claim sensitivity to new physics in these decays.

The theory of nonleptonic B decays underwent important progress in the last few years. Factorization theorems for $B \rightarrow M M^0$ decays have been proven to all orders in α_s at leading order in $\Lambda_{\text{QCD}}/\bar{m}_b$, for decays when M is a light (charmless) meson and M^0 is either charmed or charmless [1, 2, 3, 4, 5]. Here $\Lambda_{\text{QCD}} \approx 500 \text{ MeV}$ denotes a typical hadronic scale. An important difference between the various approaches to making predictions for the charmless $B \rightarrow M_1 M_2$ decay rates [2, 5, 6, 7, 8, 9, 10, 11, 12, 13] is how certain $O(\Lambda_{\text{QCD}}/\bar{m}_b)$ power suppressed corrections are treated. In particular, it was observed that so-called annihilation diagrams (as in Fig. 2) give rise to divergent convolution integrals if one attempts calculating them using conventional factorization techniques [7]. In the KLS (or pQCD) approach [7], these are rendered finite by k_\perp dependences, which effectively cut off the endpoints of the meson distribution functions. KLS found large imaginary parts from the jet scale, μ_{jet}^2 , from propagators via $\text{Im} [x \bar{m}_b^2 - k_\perp^2 + i\epsilon]^{-1} = -\pi \delta(x \bar{m}_b^2 - k_\perp^2)$ [14]. They also found that for the physical value of \bar{m}_b the power suppression of these terms relative to the leading contributions was not very significant. In the BBNS (or QCDF) approach [2, 10, 11], the divergent convolutions are interpreted as signs of infrared sensitive contributions, and are modeled by complex parameters, $X_A = \int_0^1 dy y = (1 + A e^{i\phi_A}) \ln(\bar{m}_B/\mu)$, with $A \geq 1$ and an unrestricted strong phase ϕ_A . In Ref. [15] annihilation diagrams were investigated in the soft-collinear effective theory (SCET) [16] and parameterized by a complex amplitude. When annihilation is considered in $SU(3)$ flavor analyses a complex parameter is also used [17]. In the absence of a factorization theorem for annihilation contributions, a dimensional analysis based parameterization with $\Lambda_{\text{QCD}}/\bar{m}_b$ magnitude and unrestricted strong phases is a reasonable way of estimating the uncertainty. In order not to introduce model dependent correlations, a new parameter could be used for each independent channel.

It was recently shown by Manohar and Stewart [18] that properly separating the physics at different momentum scales removes the divergences, giving well defined results for convolution integrals through a new type of factorization which separates modes in their invariant mass and rapidity. The analysis involves a minimal subtraction with the zero-bin method to avoid double counting, and with the regulation and subtraction of divergences for large p^+ and p^- momenta that behave like ultraviolet divergences. Additional subtractions would correspond to scheme dependent terms, so the minimal subtraction is the usual and sim-

plest choice. We refer to this as MS-factorization.¹ In this paper we classify annihilation contributions to $B \rightarrow M_1 M_2$ decays and demonstrate how this factorization works for the leading terms of order $\Lambda_{\text{QCD}}^2(m_b)$. By explicitly computing the matrix elements in SCET we show that leading order annihilation contributions are real, and are determined by f_B and the twist-2 distribution functions $\phi_M(x)$. We also show that a nonperturbative complex hadronic parameter first shows up for annihilation at $O(\Lambda_{\text{QCD}}^2(m_b))$.

An interesting set of power corrections are those proportional to Λ_{QCD}^2 where $\Lambda_{\text{QCD}}^2 = (m_u + m_d)$ and $\Lambda_K^2 = m_K^2 = (m_u + m_s)$ [19]. For kaons and pions $\Lambda_{\text{QCD}}^2 \sim 2 \text{ GeV}$, so corrections proportional to $\Lambda_{\text{QCD}}^2 m_b$ can be sizable, and were labeled "chirally enhanced" in Ref. [2, 10]. In the chiral limit $\Lambda_{\text{QCD}}^2 / \Lambda_{\text{QCD}}^2$, where Λ_{QCD} is the chiral symmetry breaking scale, so the enhancement is not parametric, and comes from the fact that $\Lambda_{\text{QCD}}^2 > \Lambda_{\text{QCD}}^2$. In the BBNS approach these $\Lambda_{\text{QCD}}^2 m_b$ annihilation power corrections are included along with the leading order terms, and when they multiply divergent convolutions they are described by complex parameters. Below we show that, much like the lowest order annihilation contributions, these terms are also real and factorizable.

In section II we review the leading order factorization theorem, and classify power corrections to $B \rightarrow M_1 M_2$, with a focus on annihilation amplitudes. In section III a factorization theorem is derived for local annihilation amplitudes at order $\Lambda_{\text{QCD}}^2 m_b$ for final states not involving isosinglets (given in Eq. (23)). The extension to chirally enhanced local annihilation terms is considered in section IV. In section V we study annihilation amplitudes from time-ordered products, and classify complex contributions generated at the hard scale m_b , the intermediate scale $\Lambda_{\text{QCD}}^2 m_b$, and the nonperturbative scale Λ_{QCD}^2 . Our results give absolute predictions for the annihilation amplitudes in $B \rightarrow PP; PV; VV$ channels, given the meson distribution functions as inputs, which are studied in Section VI. This section also discusses the implications of our results for models of annihilation used in the literature, and a numerical analysis of the annihilation amplitudes in $B \rightarrow K$ and $B \rightarrow KK$. Appendix A gives the derivation of a two-dimensional convolution formula with overlapping zero-bin subtractions needed for these results.

II. ANNIHILATION CONTRIBUTIONS IN SCET

We use M to denote a charmless pseudoscalar or vector meson (π, K, ρ, \dots). The relevant scales in $B \rightarrow M_1 M_2$ decays are $m_W, m_b, E, m_B=2, m_c$, the jet scale \sqrt{E} , and the nonperturbative scale Λ_{QCD} . Here E is the energy of the light mesons, which is much greater than their masses, $m_{M_{1,2}}$. To simplify notation, we denote by m_b hereafter the expansion in all hard scales, m_b, E, m_c . The decays $B \rightarrow M_1 M_2$ are mediated by the weak $B = 1$ effective Hamiltonian, which has $S = 0$ terms for $b \rightarrow d\bar{u}q_2$ transitions and

¹ Over the objection of one of the authors.

$S = 1$ terms for $b \rightarrow s q_1 q_2$. For $S = 0$ it reads

$$H_W = \frac{G_F}{\sqrt{2}} \sum_{p=u,c} V_{pb} V_{pd}^* \left[C_1 O_1^p + C_2 O_2^p + \sum_{i=3}^{10} C_i O_i \right]; \quad (1)$$

where the operators

$$\begin{aligned} O_1^u &= (ub)_{V-A} (du)_{V-A}; & O_2^u &= (ub)_{V-A} (du)_{V-A}; \\ O_1^c &= (cb)_{V-A} (dc)_{V-A}; & O_2^c &= (cb)_{V-A} (dc)_{V-A}; \\ O_3 &= \sum_{q^0} (db)_{V-A} (q^0 q^0)_{V-A}; & O_4 &= \sum_{q^0} (db)_{V-A} (q^0 q^0)_{V-A}; \\ O_5 &= \sum_{q^0} (db)_{V-A} (q^0 q^0)_{V+A}; & O_6 &= \sum_{q^0} (db)_{V-A} (q^0 q^0)_{V+A}; \\ O_7 &= \sum_{q^0} \frac{3e_{q^0}}{2} (db)_{V-A} (q^0 q^0)_{V+A}; & O_8 &= \sum_{q^0} \frac{3e_{q^0}}{2} (db)_{V-A} (q^0 q^0)_{V+A}; \\ O_9 &= \sum_{q^0} \frac{3e_{q^0}}{2} (db)_{V-A} (q^0 q^0)_{V-A}; & O_{10} &= \sum_{q^0} \frac{3e_{q^0}}{2} (db)_{V-A} (q^0 q^0)_{V-A}; \\ O_7 &= \frac{e}{8} m_b d \quad F \quad (1 + \gamma_5) b; & O_{8g} &= \frac{g}{8} m_b d \quad G^a T^a (1 + \gamma_5) b; \end{aligned} \quad (2)$$

Here $O_{1,2}^u$ and $O_{1,2}^c$ are current-current operators, and a, b are color indices, O_{3-6} are penguin operators and O_{7-10} are electroweak penguin operators, with a sum over $q^0 = u; d; s; c; b$ flavors, and electric charges e_{q^0} . Results for $S = 1$ transitions are obtained by replacing $d \rightarrow s$ in Eqs. (1) and (2), and likewise in the equations below. The coefficients in Eq. (1) are known at NLL order [20] (we have $O_1^p \pm O_2^p$ relative to [20]). In the NDR scheme, taking $\alpha_s(m_Z) = 0.118$ and $m_b = 4.3 \text{ GeV}$,

$$\begin{aligned} C_{1-10}(m_b) &= \{1.080; 0.177; 0.011; 0.033; 0.010; 0.040; \\ &\quad 4.9 \cdot 10^{-4}; 4.6 \cdot 10^{-4}; 9.8 \cdot 10^{-3}; 1.9 \cdot 10^{-3}\}; \end{aligned} \quad (3)$$

To define what we mean by annihilation amplitudes we use the contraction amplitudes $A_1, A_2, P_3, P_3^{\text{GIM}}$ in the full electroweak theory from Ref. [21] (which thus includes penguin annihilation). These amplitudes are scheme and scale independent and correspond to Feynman diagrams with a Wick contraction between the spectator flavor in the initial state and a quark in the operators O_i . Using SCET these annihilation amplitudes can be proven to be suppressed by $\sim m_b$ to all orders in α_s [5]. These contributions differ from emission-annihilation amplitudes, EA_1 and EA_2 , which involve at least one isosinglet meson. As demonstrated in Refs. [11, 22], $EA_{1,2}$ occur at leading order in the power expansion. We focus on isodoublet and isotriplet final states, so ignore the $EA_{1,2}$ amplitudes hereafter.

To separate the mass scales occurring below m_b we need to match H_W onto operators in SCET. The nonperturbative degrees of freedom are soft quarks and gluons for the B -meson, n -collinear quarks and gluons for one light meson, and \bar{n} -collinear fields for the other light meson, as defined in [23]. Expanding in α_s gives

$$\begin{aligned} \langle M_1 M_2 | H_W | B \rangle &= A^{(0)} + A_{\text{cc}} + A_{\text{ann}}^{(1)} + A_{\text{rest}}^{(1)} + \dots \\ &= \frac{G_F m_B f_{M_1} f_{M_2} f_B}{\sqrt{2}} \left[\hat{A}^{(0)} + \hat{A}_{\text{cc}} + \hat{A}_{\text{ann}}^{(1)} + \hat{A}_{\text{rest}}^{(1)} + \dots \right]; \end{aligned} \quad (4)$$

In the second line we switched to dimensionless amplitudes \hat{A} by pulling out a prefactor with the correct $\mu_b^{5=2} m_b^{1=2}$ scaling. Here $\mu_b = 500 \text{ MeV}$ represents a B -meson scale that is $O(\Lambda_{\text{QCD}})$. Taking $\mu_b = m_b$ we have the leading order amplitude $\hat{A}^{(0)} = O(\mu_b^0)$, and the subleading amplitude $\hat{A}^{(1)} = \hat{A}_{\text{ann}}^{(1)} + \hat{A}_{\text{rest}}^{(1)} = O(\mu_b^{-1})$, which we have split into the annihilation amplitude $\hat{A}_{\text{ann}}^{(1)}$ and the remainder $\hat{A}_{\text{rest}}^{(1)}$. The amplitude \hat{A}_{cc} in Eq. (4), denotes contributions from long-distance charm effects in all amplitudes, while perturbative charm loops contribute in the amplitudes $A^{(0)}$ and $A^{(1)}$.²

There are two formally large scales, m_b and μ_b , which we will refer to as the hard scale $\mu_h = m_b$, and intermediate scale $\mu_i = \mu_b$. These scales can be integrated out one-by-one [26] with effective theories SCET_I and SCET_{II}. Integrating out m_b requires matching the O_i onto a series of operators in SCET_I, $Q^{(j)}_{\text{I}}$ where the SCET_I power counting parameter $\mu_i^{1=2} = \mu_b^{1=2}$. To obtain contributions to $B \rightarrow M_1 M_2$, we require an odd number of ultrasoft (usoft) light quarks q_{ls} , two or more n -collinear fields, and two or more \bar{n} -collinear fields, where $n^2 = \bar{n}^2 = 0$.

We briefly review results from Refs. [4, 5] for the leading amplitude $A^{(0)}$ for $B \rightarrow M_1 M_2$. Here we have weak operators $Q_{1d\ 6d}^{(0)}$, $Q_{1d\ 8d}^{(1)}$ with no q_{ls} 's, taken in time-ordered products with an usoft-collinear quark Lagrangian, $L_q^{(j)}$ for $j = 1, 2$, which has one q_{ls} . We denote other subleading Lagrangians by $L^{(j)}$, and list the $O(\mu_b^{-7})$ and $O(\mu_b^{-8})$ time-ordered products for $A^{(0)}$ in Table I. Matching these time-ordered products onto SCET_{II} gives the leading $O(\mu_b^{-6})$ operators.³ When combined with the $\mu_b^{7=2}$ from the states this yields a matrix element of order $\mu_b^{5=2}$, in agreement with the prefactor in Eq. (4). Examples of the weak operators in SCET_I are

$$\begin{aligned} Q_{1d}^{(0)} &= u_{n; !_1} \not{P}_L b_v \cdot d_{\bar{n}; !_2} \not{P}_L u_{n; !_3} ; \\ Q_{1d}^{(1)} &= u_{n; !_1} \not{P}_L b_v \cdot d_{\bar{n}; !_2} \not{P}_L u_{n; !_3} ; \end{aligned} \quad (5)$$

where other $Q_{1d}^{(0;1)}$ have different flavor structures. The "quark" fields with subscripts n and \bar{n} contain a collinear quark field and Wilson line with large momenta labels $!_i$, such as

$$u_{n; !} = \not{W}_n^{(u)} (! \cdot n) \psi : \quad (6)$$

Here \not{W}_n creates a n -collinear quark, or annihilates an antiquark, $W_n = W[! \cdot n, A]$ is the standard SCET collinear Wilson line built from the n component of n -collinear gluons, \not{P} is an operator that picks out the large n label momentum of the fields it acts

² \hat{A}_{cc} has the c -fields in $O_{1,2}^c$ and O_{3-10} replaced by nonrelativistic fields [5], and is suppressed by at least their relative velocity, $v \approx 0.3-0.5$. The possibility of large nonperturbative charm loop contributions was first discussed in Refs. [12, 13], and the size of these terms remains controversial [24, 25].

³ Recall that to derive the μ_b^{-6} , we note that $\mu_b^{-8} = \mu_b^{-4}$, and changing the scaling μ_b^{-1} for four collinear quark fields in matching SCET_I to SCET_{II} gives the extra μ_b^{-2} . The μ_b^{-7} term gains an extra μ_b^{-1} from the change in scaling to a collinear D_2 .

where the f_a^M and f_b^B 's are twist-2 and twist-3, two and three parton distributions and we pulled out $f_B f_M$ for convenience. The jet functions J, J_{ab} occur due to the time-ordered product structure in SCET_I and contain contributions from the scale $\overline{p m_b}$. Using the result for \hat{J}^{BM} at order $s(i)$ this result agrees with Ref. [2] (where expressing \hat{J}^{BM} in terms of the full theory form factor generates an additional \hat{J}^{BM} term). The result for \hat{J}^{BM} is from Ref. [18] and required the MS-factorization with zero-bin subtractions. The set of contributing functions (indices a;b) is determined by the complete set of SCET_{II} operators derived in Ref. [27]. The power counting in $s(i)$ for the SCET_I functions \hat{J}^{BM} and \hat{J}^{BM} agree with that derived in pQCD [28].

Next we classify the contributions to the power suppressed $B \rightarrow M_1 M_2$ amplitudes $A^{(1)}$. In SCET_I we need to study operators and time-ordered products with scaling up to $O(10)$. These have one or three light usoft quark fields. The relevant terms are listed in Table I, where $Q_i^{(j)} \sim \overline{p}^{6+j}$ and our notation for the Lagrangians up to second order is taken from Ref. [29]. A basis for the $Q_i^{(2;3)}$ operators and the $L_q^{(3;4)}, L^{(3)}$ Lagrangians is not known, but only general properties of these operators are required for our analysis. A basis for the $Q_i^{(4)}$ operators is constructed in the next section. Dashes in Table I indicate terms that are absent to all orders in s for reasons to be explained below. To determine the perturbative order listed in the table we count the number of hard $s(h)$ factors from the matching, and the number of intermediate scale $s(i)$ factors from the SCET_I time-ordered products. The dependence in SCET_{II} column lists the nonperturbative quantities that appear in the factorization theorem for the leading order result described above, and from the factorization theorems we will derive in sections III and IV below. The properties column lists whether the nonperturbative distribution functions are complex or real as described in detail in section V, and has implications for strong phase information in the power corrections. The results in Table I imply the following power counting (for amplitudes not involving A_∞),

$$\begin{aligned} \text{Re } \hat{A}^{(0)} & \sim s(i); & \text{Im } \hat{A}^{(0)} & \sim s(i) s(h); \\ \text{Re } \hat{A}_{\text{ann}}^{(1)} & \sim s(h) + \frac{2}{s(i)} \frac{1}{m_b}; & \text{Im } \hat{A}_{\text{ann}}^{(1)} & \sim \frac{2}{s(i)} \frac{1}{m_b}; \\ \text{Re } \hat{A}_{\text{rest}}^{(1)} & \sim s(i) \frac{1}{m_b}; & \text{Im } \hat{A}_{\text{rest}}^{(1)} & \sim s(i) \frac{1}{m_b}; \end{aligned} \quad (10)$$

To facilitate the discussion we divide the contributions to annihilation amplitudes into local annihilation contributions, $A_{L\text{ann}}^{(1;2)}$ from the operators $Q_i^{(4;5)}$ that are insensitive to the jet scale, and into the remaining annihilation amplitudes, $A_{T\text{ann}}^{(1)}$, which are from time-ordered products in SCET_I. Thus,

$$A_{\text{ann}}^{(1)} = A_{L\text{ann}}^{(1)} + A_{T\text{ann}}^{(1)}; \quad (11)$$

In the literature [7, 8, 10, 11, 30] only local annihilation amplitudes have been calculated, and their matrix elements were parameterized by complex amplitudes. In SCET, $Q_i^{(4)}$ is a six-quark operator with one usoft quark, such as

$$d_s s b_v u_n; i_2 n q_n; i_3 q_n; i_1 n u_n; i_4; \quad (12)$$

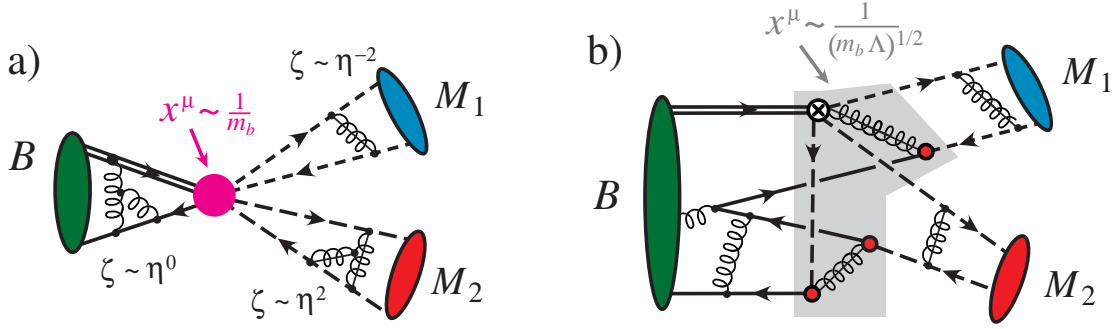


FIG. 1: The two types of factorization contributions to annihilation amplitudes which are the same order in $\alpha_s = \alpha_{\text{QCD}} = m_b$. a) shows $Q_i^{(4)}$ which has 1 hard gluon and factorizes at the scale m_b . The rapidity parameter, $\zeta = p^- p^+$ controls the MS-factorization between soft momenta (B), n-collinear momenta (M_2), and n-collinear momenta (M_1). b) shows the time-ordered product $Q_i^{(1)} [L_q^{(1)}]^3$ which factorizes at the scale $\overline{P} m_b$ and does not need a hard gluon.

where other $Q_i^{(4)}$ operators have different flavor structures. To derive the power counting for this operator, start with $Q^{(0)}$ [6], then note that switching a collinear quark to an usoft quark costs η^2 , and adding a \bar{q} and q from a hard gluon also costs η^2 . This yields $Q_i^{(4)} = O(s(\eta)^{10})$. In matching onto SCET_{II} we simply replace $Q_i^{(4)} \rightarrow O_i^{(1L)}$ [7], with the operator having an identical form. SCET_I operators $Q_i^{(4)}$ that do not have the form in Eq. (12) exist, but they must be taken in a time-ordered product with a subleading Lagrangian and so do not contribute to $A^{(1)}$. For this reason all local operator contributions to $A^{(1)}$ contribute in the annihilation terms and not in $A_{\text{rest}}^{(1)}$. Since the matching onto $O_i^{(1L)}$ is local it appears as in Fig. 1a, with an $s(\eta)$, but with no jet function. Thus this contribution to A_{ann} is of order $s(\eta) = s(i) = m_b$ relative to $A^{(0)}$. In section III we construct a complete basis of $Q_i^{(4)}$ operators and show that their matrix elements are factorizable in SCET at any order in perturbation theory, and do not generate strong phases at $O(s(\eta))$. We prove a similar theorem for chirally enhanced terms in the set $Q_i^{(5)}$ in section IV.

The annihilation amplitudes and other m_b suppressed amplitudes also occur through time-ordered products. A subset of these terms were considered in Ref. [15], including the diagram in Fig. 1b, and the phenomenological impact of these power corrections was studied. So far no attempt has been made to work out the strong phase properties and perturbative order in s of the time-ordered products, and we take up this task here. A complete classification of time-ordered products for the first order power corrections to $B \rightarrow M_1 M_2$ is listed in Table I. A subset of these terms contribute to the annihilation amplitudes as indicated in the table. To see which, we note that terms with a $Q_i^{(0;1)}$ and only one $L_q^{(1)}$ do not contribute to annihilation at either leading or next-to-leading order; the weak operator is not high enough order in η to contain an extra $n\bar{n}$ pair, and there are not enough L_q 's to produce the pair through a soft quark exchange. To rule out these

terms it was important that we are not considering isosinglet final states, which receive emission annihilation contributions already at leading order. The term $Q_i^{(2)} [L_q^{(1)}]^2$ does not contribute to annihilation because we find that all annihilation type contractions are further power suppressed when matched onto SCET_{II}. On the other hand, time-ordered products with three $L_q^{(1)}$'s or with a $Q^{(j-2)}$ do contribute to annihilation. An example of the former is shown in Fig. 1b. Compared to $Q_i^{(4)}$ shown in Fig. 1a, these time-ordered products are suppressed by $\frac{2}{s}(s_i) = s(s_h)$, and as labeled in Table I can be proven to involve a complex nonperturbative function. Thus, if perturbation theory converges rapidly at the scale s_i , then complex annihilation amplitudes are highly suppressed. If perturbation theory at s_i is poorly convergent then the time-ordered product contribution could be important numerically; comparable or even larger than the leading local annihilation amplitude from $Q_i^{(4)}$. Local annihilation contributions are discussed in detail in sections III and IV, while strong phase properties of the amplitudes and the time-ordered product contributions are taken up in section V.

III. LOCAL SIX-QUARK OPERATORS IN SCET_{II}

In this section we construct a complete basis of $O_i^{(1L)}$ operators in SCET_{II} (the $Q_i^{(4)}$ terms in SCET_I) and derive a factorization theorem for their contributions to $B \rightarrow M_1 M_2$. To find a complete basis we consider color, spin, and flavor structures that could appear when matching at any order in s . Color is simple, the six-quark operator must have $s_n n = 1 \quad 1 \quad 1$. Although operators with a T^A in one or more bilinears are allowed at this order, with the factorization properties of the leading Lagrangians and $\langle M_n M_n | \mathcal{O} | B \rangle = \langle 0 | j :: \mathcal{B}_s i | M_n j :: \mathcal{D} i | M_n j :: \mathcal{D} i$, the terms with T^A 's give vanishing matrix element between the color singlet hadronic states [1].

For spin we start by looking at chirality which is preserved by the matching at m_b . Since there is no jet function, the soft spectator quark that interpolates for the B-meson must come from the original operator in H_W , and we Fierz this field next to the b-quark field. To be definite, we take the other field from H_W to go in the n direction (in the SCET Hamiltonian we sum over $n \cdot \hat{n}$). For $O_{1-4;9;10}$ the allowed chiral structures induced in SCET by matching are $(LH)(LL)(LL)$ and $(LH)(LR)(RL)$ where L and R correspond to the handedness for the light quarks in the bilinears in the order shown in Eq. (12). We cannot assign a handedness to the heavy quark denoted here by H. For O_{5-8} we can have $(LH)(RL)(LR)$, $(LH)(RR)(RR)$, $(RH)(LL)(LR)$, and $(RH)(LR)(RR)$. A complete basis of Dirac structures for the individual bilinears is:

$$s = \quad ; \quad n = f \not{n} \not{n} \not{g} ; \quad n = f \not{n} \not{n} \not{g} : \quad (13)$$

Structures with s_5 are not needed because we have specified the handedness. Here \not{n} and \not{n} connect left and right-handed quarks, while \not{n} and \not{n} connect quarks of the same

handedness. From the basis in Eq. (13) we must construct an overall scalar using the tensors v, n, \bar{n}, g_2 , and γ_5 . $n \cdot n = 2$. We take $\gamma_5^2 = 1$, and work in a frame where $v_0 = 0$ and $n \cdot v = \bar{n} \cdot v = 1$ which makes the set $\{n, \bar{n}, v, g_2\}$ redundant. For reasons that will become apparent we pick v and $(n \cdot \bar{n})$ as our basis. The definite handedness allows us to turn any contraction involving γ_5 into a contraction with g_2 , for example $i \gamma_5 \bar{n} \not{n} = i \not{n} \bar{n}$, $\gamma_5 \not{n} = \not{n} \gamma_5$. The $(LH)(LR)(RL)$ and $(LH)(RL)(LR)$ structures can be ruled out since

$$\bar{n} \gamma_5 P_R \not{n} \gamma_5 P_L = \bar{n} \gamma_5 P_L \not{n} \gamma_5 P_R = 0 : \quad (14)$$

Noting that $\not{v} h_v = h_v$ this leaves four allowed spin structures

$$s = n \cdot \bar{n} = 1 \quad \bar{n} \not{n}; (\bar{n} \not{n}) \not{v} \not{n}; \not{n} \not{n}; \gamma_5 \not{n} \not{n} : \quad (15)$$

The last two structures have $q_b \cdot b_v$ and vanish identically for B -meson decays (they would contribute for B^0 's). Furthermore, the local annihilation operators are not sensitive to the k^+ momentum of the soft spectator quark. Thus we can use

$$h_0 \bar{q}_b \gamma_5 h_v \not{B} i = i m_B f_B ; \quad h_0 \bar{q}_b (\not{n} \not{n}) h_v \not{B} i = 0 : \quad (16)$$

Here f_B is the decay constant in the heavy quark limit. The fact that we can match onto a basis of local SCET operators of the form in Eq. (12) demonstrates to all orders in α_s that the local annihilation contributions are proportional to f_B . Using Eq. (16) the second Dirac structure in Eq. (15) is eliminated, so we do not list operators with $(\not{n} \not{n})$ in the soft bilinears below.

Next we consider the allowed flavor structures. From the operators $O_{1,2}$ we have $(ub)(dq)(qu)$, $(db)(uq)(qu)$, from $O_{4,6,7,8,9}$ we have $(db)(q^0 q)(qq^0)$, $(q^0 b)(dq)(qq^0)$, and $O_{7,10}$ give a combination of these. Thus a basis for B -decay operators is

$$\begin{aligned} O_{1d}^{(1L)} &= \frac{2}{m_b^3} q \not{d}_s P_R b_v \not{u}_{n;2} \not{n} P_L q_{n;3} \not{q}_{n;1} \not{n} P_L u_{n;4} ; \\ O_{2d}^{(1L)} &= \frac{2}{m_b^3} q \not{u}_s P_R b_v \not{d}_{n;2} \not{n} P_L q_{n;3} \not{q}_{n;1} \not{n} P_L u_{n;4} ; \\ O_{3d}^{(1L)} &= \frac{2}{m_b^3} q \not{q}^0 P_R b_v \not{q}_{n;2}^0 \not{n} P_L q_{n;3} \not{q}_{n;1} \not{n} P_L q_{n;4}^0 ; \\ O_{4d}^{(1L)} &= \frac{2}{m_b^3} q \not{q}^0 P_R b_v \not{d}_{n;2}^0 \not{n} P_L q_{n;3} \not{q}_{n;1} \not{n} P_L q_{n;4}^0 ; \\ O_{5d}^{(1L)} &= \frac{2}{m_b^3} q \not{d}_s P_R b_v \not{u}_{n;2} \not{n} P_R q_{n;3} \not{q}_{n;1} \not{n} P_R u_{n;4} ; \\ O_{6d}^{(1L)} &= \frac{2}{m_b^3} q \not{u}_s P_R b_v \not{d}_{n;2} \not{n} P_R q_{n;3} \not{q}_{n;1} \not{n} P_R u_{n;4} ; \\ O_{7d}^{(1L)} &= \frac{2}{m_b^3} q \not{q}^0 P_R b_v \not{q}_{n;2}^0 \not{n} P_R q_{n;3} \not{q}_{n;1} \not{n} P_R q_{n;4}^0 ; \\ O_{8d}^{(1L)} &= \frac{2}{m_b^3} q \not{q}^0 P_R b_v \not{d}_{n;2}^0 \not{n} P_R q_{n;3} \not{q}_{n;1} \not{n} P_R q_{n;4}^0 : \end{aligned} \quad (17)$$

Here we integrated out c and b quarks in the sum over flavors, so the remaining sums are over $q = u; d; s$ and $q^0 = u; d; s$. For the $S = 0$ effective Hamiltonian with Wilson coefficients $a_i^{(d)}(!_j)$ we use the notation

$$H_W = \frac{4G_F}{2} \sum_{n,n}^Z [d!_1 d!_2 d!_3 d!_4] \sum_{i=1}^8 a_i^d(!_j) Q_{id}^{(ann)}(!_j) : \quad (18)$$

To pull the CKM structures out of the SCET Wilson coefficients we write

$$a_i^d(!_j) = \begin{cases} \binom{(d)}{u} a_{iu}(!_j) + \binom{(d)}{c} a_{ic}(!_j) & [i = 1; 2; 3; 4]; \\ \left(\binom{(d)}{u} + \binom{(d)}{c} \right) a_i(!_j) & [i = 5; 6; 7; 8]; \end{cases} \quad (19)$$

where $\binom{(d)}{p} = V_{pb}V_{pd}$. Identical definitions for a_i^s are made by replacing $\binom{(d)}{u} \rightarrow \binom{(s)}{u}$ and $\binom{(d)}{c} \rightarrow \binom{(s)}{c}$. For $i = 5; 6; 7; 8$ only penguin operators contribute.

Next we take the $B \rightarrow M_1 M_2$ matrix element of H_W . The factorization properties of SCET yield

$$\langle M_1 M_2 | \mathcal{O}_{1d}^{(1L)} | B \rangle = \frac{2}{m_b^3} \langle M_1 | j_{n;2} | P_L q_{n;3} \rangle \langle \mathcal{O}_{1d}^{(1L)} | M_2 | j_{n;1} | P_L u_{n;4} \rangle \langle \mathcal{O}_{1d}^{(1L)} | P_R b_v | B \rangle + M_1 \otimes M_2 ; \quad (20)$$

with similar results for the other $\mathcal{O}_{id}^{(1L)}$ terms. Here the $M_1 \otimes M_2$ indicates terms where the flavor quantum numbers of the M_2 state match those of the n -collinear operator. The matrix elements in Eq. (20) are zero for transversely polarized vector mesons in agreement with the helicity counting in Ref. [30]. Equation (20) can be evaluated using Eq. (16) and

$$\begin{aligned} \langle P_{n_1}(p) | j_{n;1}^{(f)} | P_{L,R} q_{n;0}^{(f^0)} \rangle &= \frac{if_f}{2} C_{ff^0, nn_1} (n \cdot p \cdot !^0) !_P(y); \\ \langle V_{n_1}(p;") | j_{n;1}^{(f)} | P_{L,R} q_{n;0}^{(f^0)} \rangle &= \frac{if_V m_V n}{2 n \cdot p} C_{Vff^0, nn_1} (n \cdot p \cdot !^0) !_{V_k}(y); \end{aligned} \quad (21)$$

Here $f; f^0$ are flavor indices, $!_P(y)$ and $!_{V_k}(y)$ are the twist-2 light-cone distribution functions for pseudoscalars and vectors, $y = ! \cdot n$, $p = ! \cdot n$, and C_{ff^0}, C_{Vff^0} are Clebsch-Gordan coefficients. For the M_2 mesons, P_{n_2} and V_{n_2} , we have the same equation with $n \rightarrow n$, and $y \rightarrow x$. Since the $P_{L,R}$ only induce signs in the pseudoscalar matrix element, it is convenient to define

$$a_1^d = a_1^d + a_5^d; \quad a_2^d = a_2^d + a_6^d; \quad a_3^d = a_3^d + a_7^d; \quad a_4^d = a_4^d + a_8^d; \quad (22)$$

with similar definitions for a_i^s . Here $\epsilon = +1$ for PP, VV , and $\epsilon = -1$ for PV channels. Using these results, the $\mathcal{O}(\epsilon m_b)$ local annihilation amplitudes are

$$A_{Lann}^{(1)}(B \rightarrow M_1 M_2) = \frac{G_F f_B f_{M_1} f_{M_2}}{2} \int_0^1 dx dy H(x; y) M_1(y) M_2(x); \quad (23)$$

$M_1 M_2$	$H(x; y)$
$^+ , \quad ^+ , \quad ^+ , \quad ^+$ $^0 , \quad ^0 , \quad ^0 , \quad ^0_k$ $^0 0; \quad ^0 0 , \quad ^0 0$ $K^- () K^- ()^+$ $K^- () K^- ()^0$ $K^- () K^- ()^0$	$a_1^d(x; y) \quad a_4^d(y; x) \quad a_3^d(x; y) \quad a_3^d(y; x)$ $\frac{1}{2} a_2^d(x; y) + a_4^d(x; y) \quad a_2^d(y; x) \quad a_4^d(y; x)$ $\frac{1}{2} a_1^d(x; y) + a_3^d(x; y) + \frac{1}{2} a_4^d(x; y) + x \otimes y$ $a_1^d(x; y) \quad a_3^d(x; y) \quad a_3^d(y; x)$ $a_3^d(x; y) + a_3^d(y; x) + a_4^d(x; y)$ $a_2^d(x; y) + a_4^d(x; y)$
$K^- ()^0 , \quad K^- ()^0$ $^0 K^- () ; \quad ^0 K^- ()$ $^0 K^- ()^0 ; \quad ^0 K^- ()^0$ $^+ K^- () ; \quad ^+ K^- ()$	$a_2^s(x; y) + a_4^s(x; y)$ $\frac{1}{2} a_2^s(x; y) + a_4^s(x; y)$ $\frac{1}{2} a_4^s(x; y)$ $a_4^s(x; y)$

TABLE II: Hard functions for B^0 and B^- decays for the annihilation amplitude $A_{Lann}^{(1)}$ in Eq. (23). For each pair of mesons in the table, the first is M_1 and the second M_2 .

Here $H(x; y)$ are perturbatively calculable hard coefficients determined by the SCET Wilson coefficients $a_i(!_j)$. Results for different final states are listed in Table II for B^0 and B^- decays, and in Table III for B_s decays. Our derivation of the local annihilation amplitude in Eq. (23) is valid to all orders in α_s , and provides a proof of factorization for this term.

Matching at tree level, involves computing the $O(\alpha_s(m_b))$ graphs in Fig. 2 and comparing them with matrix elements of the SCET operators $Q_i^{(4)}$. Doing so we find that the Wilson coefficients $a_i(x; y)$ are

$$\begin{aligned}
a_{1u} &= \frac{C_F}{N_c^2} s(h) F(x; y) C_1 + \frac{3}{2} C_{10} ; & a_{1c} &= \frac{C_F}{N_c^2} s(h) F(x; y) \frac{3}{2} C_{10} ; \\
a_{2u} &= \frac{C_F}{N_c^2} s(h) F(x; y) C_2 + \frac{3}{2} C_9 ; & a_{2c} &= \frac{C_F}{N_c^2} s(h) F(x; y) \frac{3}{2} C_9 ; \\
a_{3u} &= \frac{C_F}{N_c^2} s(h) F(x; y) C_4 - \frac{1}{2} C_{10} ; & a_{3c} &= \frac{C_F}{N_c^2} s(h) F(x; y) C_4 - \frac{1}{2} C_{10} ; \\
a_{4u} &= \frac{C_F}{N_c^2} s(h) F(x; y) C_3 - \frac{1}{2} C_9 ; & a_{4c} &= \frac{C_F}{N_c^2} s(h) F(x; y) C_3 - \frac{1}{2} C_9 ; \\
a_5 &= \frac{C_F}{N_c^2} s(h) F(y; x) \frac{3}{2} C_8 ; & a_6 &= 0 ; \\
a_7 &= \frac{C_F}{N_c^2} s(h) F(y; x) C_6 - \frac{1}{2} C_8 ; & a_8 &= 0 ;
\end{aligned} \tag{24}$$

where $h = m_b$, $x = 1 - x$, $y = 1 - y$, with quark momentum fractions x and y as defined in Eq. (21) and shown in Fig. 2. The function F is

$$F(x; y) = \frac{1}{x^2 y} - \frac{1}{y(xy - 1)} ; \tag{25}$$

$M_1 M_2$	$H(x; y)$
$K^{(*)+}, K^{(*)+}$ $0K^{(*)0}, 0K^{(*)0}$	$a_4^d(y; x)$ $\frac{1}{2} a_4^d(y; x)$
$^{++}, ^{++}, ^{++}, ^{++}$ $^{00}; ^{00}, ^{00}$ $K^{(*)} K^{(*)+}$ $K^{(*)} 0K^{(*)0}$	$a_1^s(x; y) a_3^s(x; y) a_3^s(y; x)$ $\frac{1}{2} a_1^s(x; y) + a_3^s(x; y) + x \otimes y$ $a_1^s(x; y) a_4^s(y; x) a_3^s(x; y) a_3^s(y; x)$ $a_3^s(x; y) + a_3^s(y; x) + a_4^s(y; x)$

TABLE III: Hard functions for B_s decays for the annihilation amplitude $A_{\text{Lann}}^{(1)}$ in Eq. (23).

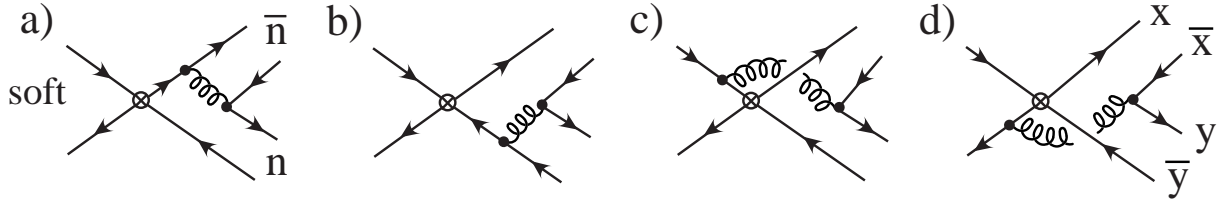


FIG. 2: Tree level annihilation graphs for $B \rightarrow M_1 M_2$ decays. Here soft, n , \bar{n} denote quarks that are soft, n -collinear, and \bar{n} -collinear respectively.

Note that our results for the coefficients $a_{3u;3c;4u;4c;7;8}$ are polluted in the sense of Ref. [5], meaning that $\mathcal{O}(\frac{2}{s})$ matching results proportional to the large coefficients $C_{1;2}$ could compete numerically. The others are not polluted: $a_{1u;2u}$ involve $C_{1;2}$ at $\mathcal{O}(s)$, while $a_{1c;2c;5;6}$ only get contributions from electroweak penguins. Our results for the diagrams in Fig. 2 agree with Refs. [7, 10], including the appearance of the combinations of momentum fractions in the functions $F(x; y)$ and $F(y; x)$. For later convenience we define moment parameters which convolute the hard coefficients with the distributions

$$\begin{aligned}
 Z_{1u}^{M_1 M_2} &= \int_0^1 dx \int_0^1 dy [a_{1u}(x; y) + a_{4+4}(x; y)] M_1(y) M_2(x); \\
 Z_{1c}^{M_1 M_2} &= \int_0^1 dx \int_0^1 dy [a_{1c}(x; y) + a_{4+4}(x; y)] M_1(y) M_2(x);
 \end{aligned} \tag{26}$$

In Eq. (25) the subscript sing denotes the fact that singular terms in convolution integrals are finite in SCET due to the MS-factorization which involves convolution integrals such as

$$\int_{x; x^0 \in 0}^Z dx_r dx_r^0 (1 - x - x^0) \frac{M(x; x^0;)}{x^2}; \tag{27}$$

where $x^{(0)}$ and $x_r^{(0)}$ correspond to label and residual momenta [18]. Implementing $x \in 0$ and $x^0 \in 0$ requires zero-bin subtractions and divergences in the rapidity must also be regulated. The δ -function sets $x^0 = 1 - x$, so $x^0 \in 0$ enforces $x \in 1$. With the usual assumption that

$\Gamma_M(x)$ vanishes at its endpoints with a power-like fall-off slower than quadratic, only integrals over $1=x^2$ in $F(x;y)$ and $1=y^2$ in $F(y;x)$ require special care. The resulting convolution integrals, $\int_0^1 dx \Gamma_M(x; \mu)$ for n -collinear and $\int_0^1 dy \Gamma_M(y; \mu)$ for n -collinear eids, are [18]

$$\begin{aligned} \int_0^1 dx \frac{\Gamma_M(x; \mu)}{(x^2)} &= \int_0^1 dx \frac{\Gamma_M(x; \mu) + x \Gamma_M^0(1; \mu)}{x^2} = \Gamma_M^0(1; \mu) \ln \frac{n}{\mu^2} ; \\ \int_0^1 dy \frac{\Gamma_M(y; \mu)}{(y^2)} &= \int_0^1 dy \frac{\Gamma_M(y; \mu) + y \Gamma_M^0(0; \mu)}{y^2} + \Gamma_M^0(0; \mu) \ln \frac{n}{\mu^2} : \end{aligned} \quad (28)$$

The moments $\int_0^1 dx \Gamma_M^i(x; \mu)$ should be considered hadronic parameters in the minimal subtraction scheme, whose value depends on μ and μ_0 and is scheme dependent beyond the usual \overline{MS} scheme for Γ_M . The dependences on μ and μ_0 are compensated by the dependences on these scales in the coefficients of SCET_{II} operators order by order in α_s . Note that the derivation of Eq. (28) includes a counterterm for an SCET_{II} operator with a $d=dp$. This operator has a real valued matrix element at any scale, which follows from the requirements discussed in section V for an SCET_{II} operator to be able to generate a physical strong phase.

Note that in deriving the result in Eq. (25) we have dropped i factors from the propagators. If these terms were kept, the second term in $F(x;y)$ would be

$$\frac{1}{(y+i)(xy-1+i)} ; \quad (29)$$

The i 's yield imaginary contributions with (y) and $(xy-1)$. They contribute for $y=0$ or for $x=y=1$, so these contributions occur in zero-bins, which are excluded from the convolution integrals in the factorization theorem we have derived with SCET. The zero-bins correspond to degrees of freedom that are soft, and including these regions would induce a double counting, so the correct factorization theorem in QCD does not include them. Factors analogous to $x \notin 0$ and $x^0 \notin 0$ in Eq. (27) ensure that there is no contribution to the integral from any zero-bin momentum, and we find that the δ -function terms give zero. This remains true for more singular distributions yielding $\Gamma^{(n)}(x)$, and so also applies to the first term in $F(x;y)$. Thus it is correct to drop the i factors from the start. This should be compared with the approach in KLS where the i factors generate a strong phase from the tree level diagrams from a k_T^2 dependent δ -function. In our derivation any such k_T^2 imaginary terms could only occur at higher orders in α_s .

Thus at order $\alpha_s(\mu_h)$ the lowest order annihilation factorization theorem is determined by the convolutions

$$\begin{aligned} \int_0^1 dx dy F(x;y) \Gamma^{M_1}(y) \Gamma^{M_2}(x) &= x^{2M_2} y^{1M_1} [y(xy-1)]^{1M_1 M_2} ; \\ \int_0^1 dx dy F(y;x) \Gamma^{M_1}(y) \Gamma^{M_2}(x) &= y^{2M_1} x^{1M_2} [x(xy-1)]^{1M_1 M_2} : \end{aligned} \quad (30)$$

where we use Eq. (28), and

$$\int_0^1 dy \frac{\Gamma_M(y; \mu)}{y} ; \quad \int_0^1 dx \int_0^1 dy f(x;y) \Gamma^{M_1}(y; \mu) \Gamma^{M_2}(x; \mu) : \quad (31)$$

These results do not have a complex phase because the right-hand side of Eq. (30) is real. Furthermore, Eq. (30) determines $A_{\text{ann}}^{(1)}$ entirely by \mathcal{M} , a function that already appears in the $A^{(0)}$ factorization theorem.

We have shown that the factorization theorem in Eq. (23) for the local contributions $O_i^{(1L)}$ yields a well-defined annihilation amplitude. At order $\alpha_s(m_b)$ the result is real, so $A_{\text{Lann}}^{(1)}$ is real up to perturbative corrections. Order $\alpha_s^2(m_b)$ corrections to the a_i will produce perturbative strong phases in $A_{\text{Lann}}^{(1)}$. Further discussion on strong phases is given in section V, while phenomenological implications are taken up in section VI.

IV. CHIRALLY ENHANCED LOCAL ANNIHILATION CONTRIBUTIONS

At order $\alpha_s(m_b) \sim m_b^2$ there are contributions from chirally enhanced operators that could compete with the $\alpha_s(m_b) \sim m_b$ terms [10]. In SCET we define these contributions as the set of SCET_{II} operators analogous to $O_i^{(1L)}$ but with an extra \not{P}_\perp between collinear quark fields. We start by constructing a complete basis for local operators at this order with a \not{P}_\perp , calling them $O_i^{(2L)}$. These operators have the same color and flavor structures as Eq. (17). The chiral structures induced from the operators O_{1-10} and the initial basis of Dirac structures shown in Eq. (15) are also the same, and allow us to eliminate many possibilities.

The complete set of Dirac structures from matching the operators $O_{1-4,9,10}$ include

$$\begin{aligned} s_n \not{P}_\perp = & \not{P}_\perp \not{P}_\perp; \not{P}_\perp \not{P}_\perp; \not{P}_\perp \not{P}_\perp; \\ & \not{P}_\perp \not{P}_\perp; \not{P}_\perp \not{P}_\perp; \end{aligned} \quad (32)$$

plus the analogous set $s_n \not{P}_\perp$. Our basis does not include operators with \not{P}_\perp^2 , because the mesons M_i have zero transverse momentum, so we can integrate these terms by parts to put them in the form in Eq. (32). The third term in Eq. (32) has chiral structure $(LH)(LR)(RL)$ and vanishes by Eq. (15). The terms in Eq. (32) all have $\not{q}_\perp \not{b}_\nu$, and so do not contribute for B-decays. The same holds if we replace \not{P}_\perp by $i\not{g}B_\perp$. Thus, at any order in perturbation theory the only $O(\alpha_s^2)$ local operator contributions from $O_{1-4,9,10}$ are those with a D_s in the soft bilinear.

For O_{5-8} we have the structures in Eq. (32), and when the q^0 flavor is a soft quark with $P_L = P_R$ Dirac structure from O_i we also have

$$\begin{aligned} s_n \not{P}_\perp = & 1 \not{P}_\perp; 1 \not{P}_\perp; \\ s_n \not{P}_\perp = & 1 \not{P}_\perp; 1 \not{P}_\perp; \end{aligned} \quad (33)$$

plus operators with 1 replaced by \not{P}_\perp , which vanish due to Eq. (16). The operators in Eq. (33) contribute to B-decays. In particular, they yield both transverse and longitudinal

polarization in $B \rightarrow VV$. A complete basis for the local $O^{(8)}$ operators with one P_γ is

$$\begin{aligned}
O_{1d}^{(2L)} &= \frac{1}{m_b^4} \bar{q} \gamma^\mu q \bar{s}^0 P_L b_V d_{n;12} \bar{n} P_L q_{n;13} q_{n;11} \bar{n} P_\gamma P_R q_{n;14}^0 ; \\
O_{2d}^{(2L)} &= \frac{1}{m_b^4} \bar{q} \gamma^\mu q \bar{s}^0 P_L b_V d_{n;12} \bar{n} P_\gamma P_R q_{n;13} q_{n;11} \bar{n} P_R q_{n;14}^0 ; \\
O_{3d}^{(2L)} &= \frac{1}{m_b^4} \bar{q} \gamma^\mu q \bar{s}^0 P_L b_V d_{n;12} \bar{n} P_\gamma P_R q_{n;13} q_{n;11} \bar{n} P_R P_\gamma q_{n;14}^0 ; \\
O_{4d}^{(2L)} &= \frac{1}{m_b^4} \bar{q} \gamma^\mu q \bar{s}^0 P_L b_V d_{n;12} \bar{n} P_L P_\gamma q_{n;13} q_{n;11} \bar{n} P_\gamma P_R q_{n;14}^0 ; \\
O_{5d \ 8d}^{(2L)} &= O_{1d \ 4d}^{(2L)} \frac{3e_q^0}{2} ;
\end{aligned} \tag{34}$$

with sums over $q; q^0 = u; d; s$. Note that the flavor structure of these operators is identical to $O_{4d}^{(1L)}$. For the electroweak penguin operators $O_{7;8}$ an additional four operators $O_{5d \ 8d}^{(2L)}$ are needed, which have the same spin-flavor structures as $O_{1d \ 4d}^{(2L)}$, but with an e_q^0 charge factor, $\bar{q} \gamma^\mu q 3e_q^0 = 2$. Again we caution that we have not considered the complete set of local m_b^2 operators, since our basis does not include three-body terms with an igB_γ , nor terms with an extra D_s soft covariant derivative. We have also not considered $O^{(M_1 \ M_2 \ m_b^3)}$ terms. All these terms are real, and it would be interesting to calculate them in the future.

The weak Hamiltonian with Wilson coefficients for the operators $O_{id}^{(2L)}$ is

$$H_W = \frac{4G_F}{2} \left(\bar{u}^{(d)} + \bar{c}^{(d)} \right) \sum_{n,m} \left[d_{1d} d_{2d} d_{3d} d_{4d} \right] \sum_{i=1}^8 a_i (!_j) O_{id}^{(2L)} (!_j) ; \tag{35}$$

Since only the penguin operators $O_{5 \ 8}$ contribute, we pulled out the common CKM factor. Matching at tree level onto the operators $O_{id}^{(2L)}$ by keeping terms linear in the γ -momenta in Fig. 2, we find

$$\begin{aligned}
a_1(x; y) &= \frac{4C_F}{N_c} s(h) C_6 + \frac{C_5}{N_c} \frac{1+x}{y^2 y x^2} + \frac{C_5}{N_c} \frac{1}{(1-xy)xy^2} ; \\
a_2(x; y) &= \frac{4C_F}{N_c} s(h) C_6 + \frac{C_5}{N_c} \frac{1+y}{y^2 x x^2} + \frac{C_5}{N_c} \frac{1}{(1-xy)x^2 y} ; \\
a_3(x; y) &= \frac{4C_F}{N_c} s(h) C_6 + \frac{C_5}{N_c} \frac{1}{y^2 x^2} + \frac{C_5}{N_c} \frac{1}{(1-xy)xy^2} ; \\
a_4(x; y) &= \frac{4C_F}{N_c} s(h) C_6 + \frac{C_5}{N_c} \frac{1}{y^2 x^2} + \frac{C_5}{N_c} \frac{1}{(1-xy)x^2 y} ; \\
a_{5 \ 8}(x; y) &= a_{1 \ 4}(x; y) \text{ with } C_5 \rightarrow C_7; C_6 \rightarrow C_8 ;
\end{aligned} \tag{36}$$

where x and y are defined in Fig. 2. These coefficients are polluted in the sense of Ref. [5], meaning that $O^{(2_s)}$ matching results proportional to the large coefficients $C_{1;2}$ could compete numerically. This makes the computation of these $O^{(2_s)}$ corrections important.

For decays involving a pseudoscalar in the final state, the operators $O_{1d}^{(2L)}$ and $O_{2d}^{(2L)}$ generate so-called "chirally enhanced" terms, proportional to Λ_{QCD}^2 . Time-ordered products of SCET_I operators also generate Λ_{QCD}^2 terms, but only at $O(\alpha_s^2)$. It is not clear that the chirally enhanced terms are larger numerically than other power corrections. In particular three-body distributions from operators with γ_5 (or $\gamma_5 \gamma_\mu$) are parametrically (and sometimes numerically as well) of similar importance [32]. The distributions are related by [33]

$$\begin{aligned} f_P^{\text{P}}(x) + \frac{(2x-1)}{x(1-x)} f_P^{\text{P}}(x) &= 6f_{3P} \frac{G_{P_z}^{(t)}(x)}{x} + \frac{G_{P_y}^{(t)}(x)}{1-x}; \\ f_P^{\text{P}}(x) - \frac{1}{6x(1-x)} f_P^{\text{P}}(x) &= f_{3P} \frac{G_{P_z}^{(t)}(x)}{x} - \frac{G_{P_y}^{(t)}(x)}{1-x}; \end{aligned} \quad (37)$$

where $G_{P_z}^{(t)}(x)$ and $G_{P_y}^{(t)}(x)$ are integrals over the three-parton distribution, f_{3P} . These relations allow certain chirally enhanced terms with f_P^{P} to be traded for non-chirally enhanced terms with f_{3P} . Thus it is clear that the chirally enhanced terms dominate over the three-body operators only in the special case when the linear combinations in the square brackets on the left-hand side of Eq. (37) are numerically suppressed. Solving with these linear combinations set to zero determines the two-body distributions f_P^{P} and f_P^{P} in the Wandzura-Wilczek (WW) approximation [34]. Thus in order to uniquely specify the f_P^{P} dependent terms, the WW approximation was needed in Ref. [10].

In contrast, in SCET we are not forced to assume a numerical dominance of the f_P^{P} terms to uniquely identify them. We can instead define local chirally enhanced annihilation terms to be the matrix elements of the operators $O_{1d}^{(2L)}$ and $O_{2d}^{(2L)}$ for final states with a pseudoscalar. The remaining terms involve other operators, and we postpone discussing them to future work. We proceed to work out the factorization theorem for $O_{1d}^{(2L)}$ and $O_{2d}^{(2L)}$ with steps analogous to Eqs. (20) through (23). To take the matrix element we need Eq. (21) and the result

$$\langle P_{n_1}(p) | j_{q_1}^{(f)} | P_{n_2}(p) \rangle = \frac{i}{6} C_{ff^0} \langle n_1 | j_{q_1}^{(f^0)} | n_2 \rangle f_P^{\text{P}}(y) : \quad (38)$$

Here C_{ff^0} are Clebsch-Gordan factors, $y = \frac{p_1 \cdot p_2}{p^2}$, and we have not written the y -dependence in the distribution due to the δ -function. The distribution $f_P^{\text{P}}(y)$ is related to more standard twist-3 two-parton and three-parton distributions by [18, 33]

$$f_P^{\text{P}}(y) = 3y f_P^{\text{P}}(y) + \frac{1}{6} f_P^{\text{P}}(y) + \frac{2f_{3P}}{f_P^{\text{P}}} \int_0^1 \frac{dy^0}{y^0} f_{3P}(y, y^0; y) : \quad (39)$$

Note that in f_P^{P} , the f_{3P} term does not have the chiral enhancement factor Λ_{QCD}^2 . There will be additional terms proportional to f_{3P} generated by three-body operators. We choose the f_P^{P} and f_{3P} basis of twist-three distributions, keeping in mind the relations in Eq. (37). For decays involving one or more pseudoscalars in the final state we find the chirally enhanced

$M_1 M_2$	$H_1(x; y)$	$H_2(x; y)$
$K^+ K^+, K^+ K^0, K^+ K^0$	$a_1(x; y) + \frac{1}{2}a_5(x; y)$	$a_2(x; y) - \frac{1}{2}a_6(x; y)$
$K^0 K^0, K^0 K^0, K^0 K^0$	$\frac{1}{2}a_1(x; y) - \frac{1}{2}a_5(x; y)$	$\frac{1}{2}a_2(x; y) + \frac{1}{2}a_6(x; y)$
$K^+ K^-, K^+ K^-, K^+ K^-$	$a_1(x; y) + \frac{1}{2}a_5(x; y)$	$a_2(x; y) - \frac{1}{2}a_6(x; y)$
$K^0 K^0, K^0 K^0, K^0 K^0$	$a_1(x; y) - \frac{1}{2}a_5(x; y)$	$a_2(x; y) + \frac{1}{2}a_6(x; y)$

TABLE V : Hard functions for the annihilation amplitude $A_{\text{Lann}}^{(2)}$ in Eq. (40) for B_s decays.

$A_{\text{Lann}}^{(2)}$. For later convenience we define moment parameters

$$\begin{aligned}
M_{1;5}^{M_1 M_2} &= \frac{1}{6} \int_0^1 dx dy a_{1;5}(x; y) M_{\text{pp}}^{M_1}(y) M_2(x); \\
M_{2;6}^{M_1 M_2} &= \frac{1}{6} \int_0^1 dx dy a_{2;6}(x; y) M_{\text{pp}}^{M_1}(y) M_2(x);
\end{aligned} \tag{41}$$

Neglecting γ_{pp} in the $W W$ approximation yields $\gamma_{\text{pp}}^P(y) = 6y(1-y)$. At order $s(\hbar)$ our results for γ_1 and γ_2 , taken with the $W W$ approximation, agree with the convolutions derived in this limit in Refs. [10, 11]. Ignoring the δ -distributions we would find that these convolution integrals diverge. The zero-bin avoided double counting in our convolutions, and yields a finite and real result for the chirally enhanced annihilation amplitude.

Let's see how this works at order $s(\hbar)$. We need two standard convolutions involving zero-bin subtractions,

$$\begin{aligned}
\int_0^1 dx dy \frac{1+x}{y^2 y x^2} M_{\text{pp}}^{M_1}(y) M_2(x) &= y^2 y^{1-M_1}_{\text{pp}} x^{2-M_2} + x^{1-M_2}; \\
\int_0^1 dx dy \frac{1+y}{y^2 x x^2} M_{\text{pp}}^{M_1}(y) M_2(x) &= x^2 x^{1-M_2}_{\text{pp}} y^{2-M_1} + y^{1-M_1};
\end{aligned} \tag{42}$$

where the y^2, y^1 moments are as in Eq. (28) and Eq. (31), and for the remaining convolution we follow Ref. [18] to find

$$y^2 y^{1-M_1}_{\text{pp}} = \int_0^1 dy \frac{M_{\text{pp}}^{M_1}(y; \epsilon)}{y^2 (1-y)} \frac{y^{M_1^0(0; \epsilon)}}{y^2} + \frac{M_{\text{pp}}^{M_1^0}(0; \epsilon)}{y^2} \ln \frac{n - M_1}{+} : \tag{43}$$

The kernels in Eq. (36) also involve two more complicated convolutions that are derived in

Appendix A ,

$$\begin{aligned}
[(1 - xy)x^2y^2]^{1 M_1 M_2}_{PP} &= \int_0^1 dx \int_0^1 dy \frac{1}{(1 - xy)x^2y^2} M_{PP}^{M_1}(y) M_{PP}^{M_2}(x) \\
&= \int_0^1 dx \int_0^1 dy \frac{M_{PP}^{M_1}(y) M_{PP}^{M_2}(x)}{(x + y - xy)x^2y^2} - \frac{M_{PP}^{M_1 0}(0) M_{PP}^{M_2}(x)}{(x + y)xy} M_{PP}^{M_1 0}(0) \int_0^1 dx \frac{M_{PP}^{M_2}(x) \ln(2 - x)}{(1 - x)^2}; \\
[(1 - xy)x^2y^2]^{1 M_2 M_1}_{PP} &= \int_0^1 dx \int_0^1 dy \frac{1}{(1 - xy)x^2y^2} M_{PP}^{M_1}(y) M_{PP}^{M_2}(x) \quad (44) \\
&= \int_0^1 dy \int_0^1 dx \frac{M_{PP}^{M_1}(y) M_{PP}^{M_2}(x)}{(x + y - xy)x^2y^2} + \frac{M_{PP}^{M_1}(y) M_{PP}^{M_2 0}(1)}{(x + y)xy} + M_{PP}^{M_2 0}(1) \int_0^1 dy \frac{M_{PP}^{M_1}(y) \ln(1 + y)}{y^2} :
\end{aligned}$$

As promised, the minimal subtraction scheme yields a well defined result for $A_{Lann}^{(2)}$. The scheme dependence cancels order by order in ϵ_s between the matrix element and perturbative corrections to the kernels obtained by matching. In any scheme the result at order $\epsilon_s(\epsilon_h)$ is real.

V. GENERATING STRONG PHASES

In this section we derive results for the order at which strong phases occur in the power suppressed amplitudes $A^{(1)}$. It is convenient to classify complex contributions to the $B \rightarrow M_1 M_2$ amplitudes according to the distance scale at which they are generated. We use the terminology *hard*, *jet*, and *nonperturbative* to refer to imaginary contributions from the scales m_b , μ_{jet} , and Λ_{QCD} respectively. We will not attempt to classify strong phases generated by charm loops, since a complete understanding of factorization for these terms order by order in a power counting expansion is not yet available.

For a matrix element to have a physical complex phase it must contain information about both final state mesons. Generically, terms in the factorized power expansion of $B \rightarrow M_1 M_2$ amplitudes involve only vacuum to meson matrix elements, so strong phase information can be contained in the Wilson coefficients or the factorized operators, but not in the states. This provides tight constraints on the source of strong phases. Nonperturbative strong phases will occur if matrix elements of these factorized operators give complex distribution functions. A necessary condition to generate a nonperturbative phase, is to have a factorized operator that is sensitive to the directions of two or more final state mesons [3], information that can be carried by Wilson lines. Physically, this is a manifestation of soft rescattering of final states. In processes like ours where soft-collinear and collinear(n)-collinear(n) factorization are relevant, this criterion implies that all strong phases reside in the soft matrix elements, where the directional information from collinear hadrons is retained in soft Wilson lines, S_r , with direction r . Since $S_r^\dagger S_r = 1$ these Wilson lines often cancel, but for many of the power suppressed terms listed in Table I the cancellation is not complete. This mechanism for generating a strong phase was first observed for $B^0 \rightarrow D^0 \bar{D}^0$ [3], where a nonperturbative

soft matrix element occurs through four-quark operators depending on n and v^0 (which are null and time-like vectors for the final state light and charmed mesons, respectively).

For the $B \rightarrow M_1 M_2$ decays with two energetic light mesons, a nonperturbative strong phase requires a soft matrix element depending on the S_n and S_n Wilson lines in SCET_{II}. The simplest way to obtain the Wilson lines for the soft operators is to match SCET_I onto SCET_{II} [26]. In SCET_I one first uses the decoupling field redefinition on collinear fields [16], $\psi_n \rightarrow Y_n \psi_n$, $\bar{\psi}_n \rightarrow Y_n \bar{\psi}_n$, $A_n \rightarrow Y_n A_n Y_n^\dagger$ and $A_n \rightarrow Y_n A_n Y_n^\dagger$, which generates the Wilson lines and factorizes usoft and collinear fields. The fields of a given type are then grouped together by Fierz rearrangements. Matching the resulting operators or time-ordered products onto SCET_{II} gives $Y_r \rightarrow S_r$, and we can read off which soft Wilson lines are present. Because of the properties of the subleading SCET_I operators, we will not have an S_n and S_n in the final SCET_{II} operator unless we have a subleading SCET_I Lagrangian with an n -collinear field and usoft fields, and one with n -collinear fields and usoft fields. We used this property to determine which entries are real or complex, and listed the results in the last column of Table I. The complex entries with multiple $L_q^{(j)}$'s [35] also have at least two hard-collinear gluons, and so generate contributions that start at $s(i)^2$ when matched onto SCET_{II}.

To determine the perturbative order of the complex contributions, we must also classify which hard and jet coefficients give complex phases. In general any hard coefficient generated by matching at 1 loop will give imaginary contributions, since these loops involve fields for both final state mesons, as pointed out for the general case in Ref. [2] and for charm loops in Ref. [36]. Since all leading order contributions in Table I have at least one $s(i)$, the hard imaginary contributions for $A^{(0)}$ are $O[s(i)s(h)]$. At order m_b all annihilation contributions but $Q_i^{(4)}$ have at least one $s(i)$, and for these terms the hard complex contributions involve $s(i)s(h)$ and thus are smaller than the nonperturbative terms proportional to $s(i)^2$. For $Q_i^{(4)}$ the amplitude is real at the leading perturbative order, $s(h)$, as demonstrated in section III, and so hard complex contributions start at $s(h)^2$. In contrast for the amplitude $A_{\text{rest}}^{(1)}$ a complex amplitude is generated at order $s(i)m_b$, which is only suppressed by m_b compared to $A^{(0)}$.

Finally, we should examine complex contributions from the jet scale. At leading order there is a unique jet function J [5]. J also contributes to the heavy-to-light form factors and only knows about the n -collinear direction. Thus $A^{(0)}$ does not get imaginary contributions at any order in the $s(i)$ expansion (which has been demonstrated explicitly to $s(i)^2$ [37]). At next-to-leading order in the power expansion, there is no known relation of the power suppressed jet functions with analogous jet functions in the form factors. However, the subleading jet functions also depend only on one collinear direction, and do not carry information about both final state mesons that could generate a physical strong phase. We demonstrate this fact more explicitly by examining the calculation at $O(s(i))$, which is sufficient to see that the amplitudes are real up to the order where a nonperturbative phase first occurs. At this order the jet functions are generated by matching tree level SCET_I

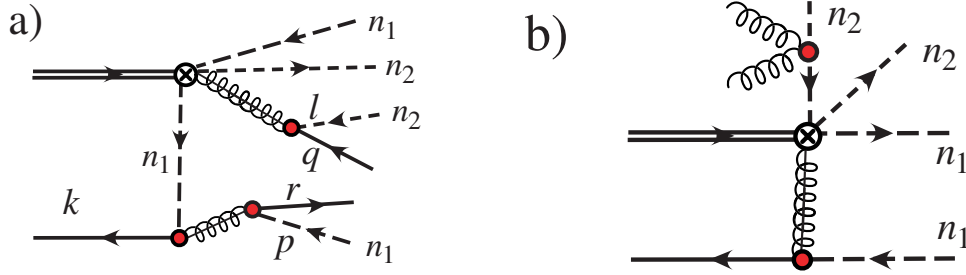


FIG. 3: Graphs which generate a strong phase in lowest order matching of SCET_I operators onto SCET_{II}: a) has a $Q^{(1)}$, two $L_{n_1 q}^{(1)}$, and one $L_{n_2 q}^{(1)}$ and contributes to the annihilation amplitude at $O(s^{-1})$; and b) has a $Q^{(1)}$, one $L_{n_1 q}^{(1)}$, and one $L_{n_2 n_2}^{(2)}$ and contributes to non-annihilation amplitudes at $O(s^{-1})$. Dashed quark lines are n_1 or n_2 collinear, and solid quark lines are soft.

diagrams onto SCET_{II}. A typical example is

$$\frac{1}{(x + i)(k^+ + i)}; \quad (45)$$

where x is a momentum fraction that will be convolved with a collinear distribution function, and the k^+ will be convolved with a soft distribution function. These jet functions are real if and only if we can drop the i factors. However, just as in section III, the i terms can be dropped because the zero-bin subtractions [18] ensure that this does not change the convolution.⁴ Thus factorization gives real $O(s^{-1})$ jet functions.

This demonstrates that complex contributions in the power suppressed annihilation amplitudes are suppressed,

$$\text{Im} \frac{A_{\text{ann}}^{(1)}}{A^{(0)}} = O\left(\frac{s^{-1}}{m_b}\right) + O\left(\frac{1}{m_b^2}\right); \quad (46)$$

On general grounds one might have expected $O(=m_b)$ suppressed strong phases, which we have demonstrated are absent in $A_{\text{ann}}^{(1)}$, though they do occur in $A_{\text{rest}}^{(1)}$.

We close this section by giving two examples of time-ordered products generating the nonperturbative strong phases discussed above. We consider a time-ordered product with three $L_q^{(1)}$ insertions contributing to annihilation. When matching onto SCET_{II} we integrate out the hard-collinear modes, leading to an eight-quark operator. Figure 3a shows the order s^{-1} contribution to this matching. The soft quark lines remain open as their contraction leads to an on-shell line which must be treated nonperturbatively. The resulting SCET_{II} operator has the generic form

$$O^{\text{II}} = J(n_2, p; n_l, r; n_q, k) \quad (47)$$

$$(qS_{n_1})_{n_1, r}^{(1)} (S_{n_2, q}^Y q)_{n_2, q} (qS_{n_2})_{n_1, k}^{(2)} (S_{n_1, l}^Y h_v) (q_{n_1, l})^{(3)} (q_{n_1, l^0})^{(4)} (q_{n_2, p^0})^{(4)} (q_{n_2, p})^{(4)}$$

⁴ A equivalent physical argument for dropping the i factors was given in Ref. [3], where it was needed to prove that certain long-distance contributions are absent in color suppressed decays.

where we use the shorthand subscript notation, $(S_{n_1}^Y q_s)_{n_1 q} = [(n_1 q)_{in P}] S_{n_1}^Y q_s$. We took the jet directions to be n_1 and n_2 , rather than n and n , to emphasize that the soft operator is sensitive to the relative directions of the jets. The functions S_i shown in Table I are defined by the matrix element of this type of operator

$$S_i(n_1 k; n_r; n_q; i) = h_0 j(q_{n_1})_{n_1 r i}^{(1)} (S_{n_2}^Y q_s)_{n_2 q} (q_s S_{n_2})_{n_1 k i}^{(2)} (S_{n_1}^Y h_v) \beta(v) i; \quad (48)$$

where i runs over color, Dirac, and flavor structures. To count the factors of α_s in these amplitudes, note that the hard-collinear contractions give g^4 , and that the matrix element of the resulting four-quark operator, $h_0 j(q:::q)(q:::b_v) \beta i$, is suppressed by $1=(4)^2$ relative to $h_0 j(q:::b_v) \beta i$. (The four-quark operator has an extra loop with no extra couplings.) This demonstrates that nonperturbative complex contributions first occur at order $[\alpha_s(i)]^2 = \alpha_s(m_b)$, i.e., suppressed by $[\alpha_s(i)] = \alpha_s(m_b)$ compared to the leading amplitudes. The phases arising from the type of matrix element shown in Eq. (48) play a crucial role in explaining the observed strong phases which arise in color suppressed decays [3]. Their resulting operators predict the equality of amplitudes and strong phases between decays involving D and D^* mesons and have been confirmed in the data [38]. This type of diagrams also have long-distance contributions of the same order, which arise from time-ordered products in SCET_{II} and can also be complex. To see this note that the hard-collinear quark propagator in Fig. 3a could also be on-shell (i.e., have $O(1)$ virtuality), in which case it would remain open until the matrix element is taken at the low scale. By opening that line we see that this contribution corresponds to the time-ordered product of a four-quark operator and a six-quark operator, both of which are generated when matching onto SCET_{II}. A long-distance part is the same order in $\alpha_s(i)$ and does not change our conclusions about these terms. In Fig. 3b we show a non-annihilation contribution to $\hat{A}_{rest}^{(1)}$ which is of order $\alpha_s(i) = \alpha_s(m_b)$. This term is generated by the time-ordered product of $Q^{(1)}$, an insertion of the n_1 -collinear $L_q^{(1)}$, and an operator with n_2 -collinear quarks and usoft gluons,

$$L^{(2)} = (n_W) Y_{n_2}^Y i \not{D}_{us}^? i \not{D}_{us}^? Y_{n_2} \frac{F}{2P} (W^Y n) : \quad (49)$$

VI. APPLICATIONS AND CONCLUSION

A. Phenomenological Implications

To understand the implications of the experimental data, it is crucial to know which contributions to the $B \rightarrow M_1 M_2$ amplitudes can be complex. The best sensitivity to non-SM physics is via interference phenomena, where new interactions enter linearly (instead of quadratically), such as CP-violating observables. The sensitivity to such effects depends on how well we understand the dominant and subdominant SM amplitudes, including their strong phases. The existence of strong phases in B decays is experimentally well established

(e.g., the $B \rightarrow D$ and $B \rightarrow D^*$ rates, the CP asymmetry A_{K^+} , the transversity analysis in $B \rightarrow J/\psi K$, etc.).

One example of how strong phase information can be useful is the method for determining from $B \rightarrow D^* K$ proposed in Ref. [39]. The method uses isospin, the factorization prediction that $\text{Im}(C=T) = 0$ at $s(m_b)$; $\Rightarrow m_b$, and does not require data on the poorly measured direct CP asymmetry C_{00} .⁵ The phases in $A^{(0)}$ at $s(m_b)$ $s(s_i)$ are calculable and partially known [2, 40]. The current $B \rightarrow D^* K$ data is in mild conflict (at the 2 level) with the SM CKM fit [41]. More precise measurements are needed to understand how well the theoretical expectations are satisfied, and to decipher whether there might be a hint for new physics. Obviously further information about power corrections in $\text{Im}(C=T)$ could help to clarify the situation.

In all factorization-based approaches to charmless B decays, several parameters are fit from the data or are allowed to vary in certain ranges. The choice and ranges of these parameters should be determined by the power counting. This motivated keeping the charm penguin amplitudes, A_{cc} as free parameters in SCET [5], as was done earlier in Ref. [12]. In the BBNS approach these are argued to be factorizable [2]. A fit to the data using this parameterization found large power suppressed effects [42] including annihilation amplitudes, which might be interpreted as a breakdown of the $\Rightarrow m_b$ expansion. In QCD sum rules, the annihilation amplitude was found to be of the expected magnitude and to have a sizable strong phase [43].

Channels like $B \rightarrow K$ and $B \rightarrow K K$ are sensitive to new physics, but by the same token are dominated by penguin amplitudes, which can have charm penguin, annihilation, and other standard model contributions. Since there are possible large nonperturbative c -loop contributions in A_{cc} that have the same $SU(3)$ flavor transformation properties as annihilation terms, they cannot be easily distinguished by simple fits to the data. However, in a systematic analysis based on SCET these correspond to different operators' matrix elements, so it is possible to disentangle the various contributions and determine their expected size. The factorization theorems for annihilation amplitudes derived here only involve distributions that already occurred at leading order. This means that we can compare the size of annihilation amplitudes to experimental data without further ambiguities from additional hadronic parameters. We take up this comparison in section VIB below.

As an explicit example of how to assemble our results in sections III and IV, we derive the local annihilation amplitude for $B^0 \rightarrow K^+ K^-$. From Table II we can read off the result for this channel, $H(x; y) = a_4^s(x; y) - a_8^s(x; y)$, and from Table IV, $H_1 = a_1(x; y) + 1 = 2a_5(x; y)$ and $H_2 = a_2(x; y) - 1 = 2a_6(x; y)$. With the lowest order matching results in Eqs. (24) and (36) we can set $a_8 = 0$ and $a_{4u} = a_{4c}$, which inserted into Eqs. (23) and (40)

⁵ Here C and T are isospin amplitudes defined in the t -convention, where t is eliminated from the amplitudes in favor of c and u .

gives

$$\begin{aligned}
A_{\text{Lann}}^{(1)}(K^+ &) = \frac{G_F f_B f f_K}{P \frac{2}{2}} \left(\binom{(s)}{c} + \binom{(s)}{u} \right) \int dx dy \binom{(1)}{4u} a_u(x; y) \binom{(y)}{K} \binom{(x)}{K} \\
&= \frac{G_F f_B f f_K}{P \frac{2}{2}} \left(\binom{(s)}{c} + \binom{(s)}{u} \right) \binom{(K)}{4u}; \\
A_{\text{Lann}}^{(2)}(K^+ &) = \frac{G_F f_B f f_K}{6 \frac{2}{2}} \left(\binom{(s)}{c} + \binom{(s)}{u} \right) \int dx dy \frac{h}{m_b} \binom{n}{o} a_1(x; y) + \frac{1}{2} a_5(x; y) \binom{o}{pp} \binom{(y)}{K} \binom{(x)}{K} \\
&\quad + \frac{K}{m_b} \binom{n}{o} a_2(x; y) \frac{1}{2} a_6(x; y) \binom{i}{pp} \binom{(y)}{K} \binom{(x)}{K} \\
&= \frac{G_F f_B f f_K}{P \frac{2}{2}} \left(\binom{(s)}{c} + \binom{(s)}{u} \right) \frac{h}{m_b} \binom{n}{K} + \frac{1}{2} \binom{o}{K} + \frac{K}{m_b} \binom{n}{K} \frac{1}{2} \binom{o}{K} :
\end{aligned} \tag{50}$$

Thus, both the leading order annihilation amplitude $A_{\text{Lann}}^{(1)}$, and the chirally enhanced annihilation amplitude $A_{\text{Lann}}^{(2)}$ are determined by the $\binom{(s)}{c}$'s defined in Eqs. (26) and (41). Other K^+ channels have similar expressions with different Clebsch-Gordan coefficients. To see explicitly what the $\binom{(s)}{c}$'s involve we insert the $O(\binom{(s)}{c})$ values of $a_{3u}(x; y)$, $a_1(x; y)$, and $a_2(x; y)$ to give

$$\begin{aligned}
A_{\text{Lann}}(K^+ &) = \frac{G_F f_B f_{M1} f_{M2}}{P \frac{2}{2}} \left(\binom{(s)}{c} + \binom{(s)}{u} \right) \frac{4}{9} \binom{(h)}{s} \\
&\quad \frac{C_9}{6} \frac{C_3}{3} \binom{h}{x} \binom{2}{K} \binom{y}{1} \binom{i}{[y(xy-1)]^{1-K}} \\
&\quad \frac{2}{3m_b} C_6 \frac{C_8}{2} + \frac{C_5}{3} \frac{C_7}{6} \binom{h}{y} \binom{2}{y} \binom{1}{pp} \binom{x}{K} + \binom{x}{1-K} \\
&\quad \frac{2}{3m_b} \frac{C_5}{3} \frac{C_7}{6} [(1-xy)xy]^{1-K} \binom{i}{pp} + \frac{2}{3m_b} \frac{C_5}{3} \frac{C_7}{6} [(1-xy)x^2y]^{1-K} \binom{i}{pp} \\
&\quad \frac{2}{3m_b} \frac{K}{C_6} \frac{C_8}{2} + \frac{C_5}{3} \frac{C_7}{6} \binom{h}{y} \binom{2}{y} + \binom{y}{1} \binom{x}{1} \binom{2}{K} \binom{i}{pp} :
\end{aligned} \tag{51}$$

Here results for the convolutions denoted by brackets $\binom{i}{h}$ can be found in Eqs. (28), (31), (43), and (44) in the minimal subtraction scheme. Model independent results for other channels can be assembled in a similar fashion. Corrections to the result in Eq. (51) are suppressed by $O[\binom{2}{s}(\binom{(s)}{c} - \binom{(s)}{m_b})]$, while we caution that additional $\binom{(s)}{h} = m_b$ terms without a $\binom{(s)}{c}$ or $\binom{(s)}{u}$ will be present in the last two lines. In the next subsection we derive results for all of these channels using a simple model for the distribution functions, and study numerically the size of the annihilation amplitudes.

Annihilation contributions have been claimed to play important roles in several observables [7, 8, 10, 11, 30], in particular in generating large strong phases in $B \rightarrow K$ decays [7, 8]. The $B \rightarrow K$ and K data indicate that the latter decays are dominated by penguin amplitudes, and the pattern of rates and CP asymmetries is not in good agreement with some predictions. In particular, it is not easy in the BBNS analysis to accommodate the measured CP asymmetry, $A_{K^+} = 0.108 \pm 0.017$ [31], except in the S3 and

S4 models of Ref. [11]. In these models the annihilation contributions are included by using asymptotic distributions, and divergent integrals are parameterized as $\int_0^1 dx x^{\alpha_A} \ln x = x^{\alpha_A} \ln x + \frac{1}{\alpha_A}$ and $\int_0^1 dx \ln x = x^2 \ln x + \frac{1}{2}$, with $X_A = (1 + \alpha_A e^{i\phi_A}) \ln(m_B = 500 \text{ MeV})$. Model S3 postulates $\alpha_A = 1$, $\phi_A = 45^\circ$ for all final states, while in the S4 scenario $\alpha_A = 1$ and $\phi_A = 55^\circ; 20^\circ; 70^\circ$ for the $PP; PV; VP$ channels, respectively. Thus

$$\text{S3: } X_A = 4.0 - 1.7i; \quad \text{S4: } X_A = f3.7 - 1.9i; 4.6 - 0.8i; 3.2 - 2.2ig: \quad (52)$$

In addition, $\alpha_s(\mu)$ and the Wilson coefficients are evaluated at the μ_i intermediate scale [11].

Our result for the factorization of annihilation contributions derived in Sec. III constrains models of annihilation. Equation (23) gives a well defined and real amplitude at leading order, which depends only on the twist-2 distributions, ϕ_M . It does not involve model parameters α_A and ϕ_A . For $A_{L_{\text{ann}}}^{(1)}$ using Eq. (28) and the asymptotic form of the meson distributions, we find a correspondence

$$\text{Re} X_A = 1 + \int_0^1 dx \frac{(x)}{6(x^2)} = \ln \frac{m_b}{\mu_+} : \quad (53)$$

Clearly, X_A is real. The asymptotic distributions $\phi_M(x) = 6x(1-x)$ are more accurate for large scales, and at the matching scale where $\mu_+ = m_b$, X_A is not enhanced by a large logarithm. We estimate $|\text{Im} X_A| < 1$. Thus, the modeling of annihilation contributions with complex X_A in the BBNS approach (including the phenomenologically favored S3 and S4 scenarios) are in conflict with the heavy quark limit, and should be constrained to give smaller real X_A 's.

In the KLS [7] treatment of annihilation, complex amplitudes are generated from dynamics at the intermediate scale from the i in propagators. The MS-factorization used in the derivation of our annihilation amplitudes demonstrates that including the i term in collinear factorization would induce a double counting. Thus we expect such contributions to physical strong phases to be realized by operators with soft exchange that occur at higher order in $1/m_b$ and therefore to be small.

Annihilation contributions were also argued to play an important role in explaining the large transverse polarization fraction in $B \rightarrow K$ [30]. It was shown that factorization implies $R_T = O(1/m_b^2)$, where R_T denotes the transverse polarization fraction [30]. Subsequently, it was shown using SCET that R_T is power suppressed unless a long-distance charm penguin amplitude A_{cc} spoils this result [5, 22]. Experimentally, one finds $R_T(B \rightarrow K) \approx 0.5$ [31], while $R_T(B \rightarrow \pi)$ is at the few percent level. It has been argued that the large $R_T(B \rightarrow K)$ may provide a hint of new physics in the $b \rightarrow sss$ channel. In Ref. [30] it was suggested that standard model annihilation contributions may account for the observed large value of $R_T(B \rightarrow K)$. Our analysis in Sec. IV agrees with [30] in that annihilation contributions to the transverse polarization amplitude at first order in $1/m_b$ are suppressed by not one, but two powers of $1/m_b$. However, we do not find a numerical enhancement of these terms (which in [30] is partly due to the large sensitivity

of the $(2X_A - 3)(1 - X_A)$ function to $\%_A$ in the BBNS parameterization). The operators in Eq. (34) give rise to transverse polarization, but since MS-factorization renders the naively divergent convolutions finite, these power suppressed amplitudes do not receive sizable enhancements. Although we have not derived explicit results for the $B \rightarrow K$ annihilation amplitudes (since π is an isosinglet), our results make it unlikely that local annihilation can explain the $R_T(B \rightarrow K)$ data. We have not explored whether the time-ordered products at $O(\frac{2}{s}(1 - m_b))$ could give rise to transverse polarization, and it would be interesting to do so.

B. Annihilation amplitudes with simple models for $\mathcal{M}_u(x)$ and $\mathcal{M}_{pp}^M(x)$

In this section we derive numerical results for the local annihilation amplitudes in various channels using a simple model for the distributions. It is convenient to write the $S = 0$ annihilation amplitude as

$$A_{L, \text{ann}}(B \rightarrow M_1 M_2) = \frac{G_F f_B f_{M_1} f_{M_2}}{2} \left[h_u^{(d)}(B \rightarrow M_1 M_2) + h_c^{(d)}(B \rightarrow M_1 M_2) + \left(h_u^{(d)} + h_c^{(d)} \right) \frac{M_1}{m_b} h_1(B \rightarrow M_1 M_2) + \frac{M_2}{m_b} h_2(B \rightarrow M_1 M_2) \right] : \quad (54)$$

For $S = 1$ decays we replace $h_{u,c}^{(d)} \rightarrow h_{u,c}^{(s)}$. The coefficients h_u, h_c, h_1 , and h_2 are equal to linear combinations of $a_{iu}, a_{ic}, a_{1,5}$, and $a_{2,6}$ with Clebsch-Gordan coefficients determined from Tables II, III, IV, V. The combinations are simply determined by the replacements

$$\begin{aligned} h_u &= H(x; y) \text{ with } a_i^{d;s}(x; y) \rightarrow a_{iu}^{d;s}(x; y) ; \\ h_c &= H(x; y) \text{ with } a_i^{d;s}(x; y) \rightarrow a_{ic}^{d;s}(x; y) ; \\ h_1 &= H_1(x; y) \text{ with } a_{1,5}(x; y) ; \\ h_2 &= H_2(x; y) \text{ with } a_{2,6}(x; y) ; \end{aligned} \quad (55)$$

For the coefficients $a_{3u;3c;4u;4c;7;8}$ and the a_i 's, the $O(\frac{2}{s}C_{1;2})$ matching corrections could be comparable numerically with the $O(\frac{2}{s}C_{3-10})$ corrections considered here. This should be kept in mind when examining numbers quoted below for the corresponding \mathcal{M} 's.

Model independent results for the coefficients a_{iu}, a_{ic} , and a_i , can be found in Eqs. (26) and (41). To derive numerical results we need to model the meson distribution functions. We take the C_i from Eq. (3), use

$$\begin{aligned} s(h) &= 0.22 ; & (h) &= 2.3 \text{ GeV} ; & K(h) &= 2.7 \text{ GeV} ; \\ f_K &= 0.16 \text{ GeV} ; & f &= 0.13 \text{ GeV} ; & f_B &= 0.22 \text{ GeV} ; \end{aligned} \quad (56)$$

where f_B comes from a recent lattice determination [44], and $h = m_b = 4.7 \text{ GeV}$. For the \mathcal{M} 's we take simple models with parameters a_i^M and a_{ipp}^M which we consider specified at the

high scale μ_h ,

$$\begin{aligned} M(x) &= 6x(1-x)^2 + a_1^M(6x-3) + 6a_2^M(1-5x+5x^2); \\ P_{pp}(x) &= 6x(1-x)^2 + a_{1pp}^P(6x-3) + 6a_{2pp}^P(1-5x+5x^2); \end{aligned} \quad (57)$$

Based on recent lattice data for moments of the π and K distributions [45] we take $a_2^{KK} = 0.2 \pm 0.2$, where the lattice error was doubled to give some estimate for higher moments. For the π we set $a_1 = a_{1pp} = 0$, while for the K we use [45] $a_1^K = 0.05 \pm 0.02$. We also take $a_{2pp}^{KK} = 0 \pm 0.4$ and $a_{1pp}^K = 0.0 \pm 0.2$. Note that the range for our parameters is similar to those used in the BBNS models [10, 11] and light-cone sum rules [46]. Since the uncertainties in the model parameters are large and not significantly affected by variation of the μ scales we keep these fixed at μ_b . A scan over models with parameters in these limits gives absolute predictions for the annihilation coefficients. For the $B \rightarrow K$ channels we find

$$\begin{aligned} R_{2u}^K &= 1.8 \pm 1.2; & R_{4u}^K &= R_{4c}^K = 0.15 \pm 0.10; & R_{2c}^K &= 0.14 \pm 0.09; \\ R_1^K &= 0.0 \pm 0.65; & R_2^K &= 0.0 \pm 0.58; & R_5^K &= 0.0 \pm 0.094; & R_6^K &= 0.0 \pm 0.11; \end{aligned} \quad (58)$$

Using these numbers we can compare the size of the local annihilation amplitudes to the $B \rightarrow K$ data,

$$\begin{aligned} R_A(K^+) &= \frac{\tilde{A}_{Lann}^{(1)}(K^+) + A_{Lann}^{(2)}(K^+)}{\tilde{A}_{\text{ExptPenguin}}(K^+)} = 0.11 \pm 0.09; \\ R_A(K^0) &= \frac{\tilde{A}_{Lann}^{(1)}(K^0) + A_{Lann}^{(2)}(K^0)}{\tilde{A}_{\text{ExptPenguin}}(K^0)} = 0.12 \pm 0.09; \end{aligned} \quad (59)$$

For the numerator we did a Gaussian scan using the values from Eq. (58), and determined the error by the standard deviation. For the denominator we used the experimental penguin amplitude determined by a fit to the $B \rightarrow K$ data in Ref. [6]. These values of R_A indicate that a fairly small portion of the measured penguin amplitude is from annihilation. We do not quote values for the ratio $A_{Lann}^{(2)} = A_{Lann}^{(1)}$, since each of the numerator and denominator can vanish and the parametric uncertainties are very large. For typical values of the parameters in the K channels we find that the $A_{Lann}^{(2)}$ is comparable or even larger than $A_{Lann}^{(1)}$ in agreement with Ref. [10]. The size of the annihilation amplitudes in Eq. (59) are consistent with our expectation for these power corrections. For $B \rightarrow KK$ we find

$$\begin{aligned} R_{1u}^{KK} &= 9.6 \pm 6.2; & R_{2u}^{KK} &= 1.7 \pm 1.1; & R_{3u}^{KK} &= R_{3c}^{KK} = 0.63 \pm 0.37; \\ R_{4u}^{KK} &= R_{4c}^{KK} = 0.14 \pm 0.09; & R_{1c}^{KK} &= 0.03 \pm 0.02; & R_{2c}^{KK} &= 0.13 \pm 0.08; \\ R_{3u}^{KK} &= R_{3c}^{KK} = 0.63 \pm 0.37; & R_1^{KK} &= 0.0 \pm 0.65; & R_2^{KK} &= 0.0 \pm 0.55; \\ R_5^{KK} &= 0.0 \pm 0.095; & R_6^{KK} &= 0.0 \pm 0.11; \end{aligned} \quad (60)$$

Using these results to determine the $c^{(d)}$ annihilation contributions to $B \rightarrow KK$ and comparing this to the experimental penguin amplitude from Ref. [6] gives

$$R_A(KK^0) = \frac{\tilde{A}_{Lann}^{(1)}(KK^0) + A_{Lann}^{(2)}(KK^0)}{\tilde{A}_{\text{ExptPenguin}}(KK^0)} = 0.15 \pm 0.11; \quad (61)$$

This is similar in size to the ratios $R_A(K^+)$, $R_A(K^0)$ and so also consistent with a power correction.

C. Conclusions

In summary, we exhibited how a new factorization in SCET renders the annihilation and "chirally enhanced" annihilation contributions finite in charmless nonleptonic $B \rightarrow M_1 M_2$ decays to non-isosinglet mesons. We constructed a complete basis of SCET_{II} operators for local annihilation contributions as well as factorization theorems valid to all orders in α_s . By matching the full QCD diagrams onto SCET_{II} operators we showed that their matrix elements are real at leading order in α_s and $\alpha_s(m_b)$. The lowest order annihilation contributions do not introduce new parameters beyond those that occur in the leading order factorization theorem, i.e., with a minimal subtraction scheme we derived absolute predictions for them in terms of f_B and $M_{1/2}$. Chirally enhanced local annihilation contributions depend in addition on $\frac{M_{1/2}}{m_b}$. The annihilation contributions can only have an unsuppressed complex part at $O(\alpha_s)$ if perturbation theory at the intermediate scale, $\frac{P}{m_b}$, breaks down.

In the previous literature models for the power suppressed annihilation corrections were often found to give enhanced contributions with large strong phases, and such assumptions have been important in some fits to the data. Considering all power suppressed amplitudes not involving charm loops, we proved that complex annihilation contributions only occur suppressed by $\alpha_s \frac{P}{m_b} \sim \alpha_s \frac{P}{m_b} \sim \alpha_s \frac{P}{m_b} \sim \alpha_s \frac{P}{m_b}$ compared to the leading amplitudes. From our factorization theorem we found that annihilation contributes (11–9)% of the penguin amplitude in $B^0 \rightarrow K^+$, (12–9)% in $B \rightarrow K^0$, and (15–11)% in $B \rightarrow K K^0$. We anticipate that our results will guide future fits to the vast amount of data on charmless B decays, and yield a better understanding of what this data means.

Acknowledgments

This work was supported in part by the Director, Office of Science, Offices of High Energy and Nuclear Physics of the U.S. Department of Energy under the Contract DE-AC02-05CH11231 (Z.L.), the cooperative research agreement DOE-FC02-94ER40818 (C.A. and I.S.), and DOE-ER-40682-143 and DEAC02-6CH03000 (I.R.). I.S. was also supported in part by the DOE OJI program and by the Sloan Foundation.

APPENDIX A : ZERO-BIN SUBTRACTIONS FOR A TWO-DIMENSIONAL DISTRIBUTION

In this appendix we derive a result for the action of the zero-bin subtractions on the integrand obtained from the chirally enhanced annihilation computation, shown in Eq. (44). Since the result involves a correlation in the x and y integrals it cannot be read off from the results in Ref. [18]. It is convenient to write the momentum fraction factor coming from the on-shell b -quark propagator as $(1 - xy) = (x + y - xy)$. Including the rapidity convergence factors [18], the integral we need is

$$I = \int_{x \in 1; y \in 0}^X \int_{-Z}^Z dx_r dy_r \frac{M_{pp}^{(1)}(y) M^{(2)}(x)}{(x + y - xy)xy^2} x - y j(x) j(y) \frac{1}{n - 1} \frac{1}{m - 2} p^2; \quad (A1)$$

where $x = (x) (1 - x)$. To determine the subtraction terms we must look at the singular behavior as we scale towards the $x = 1$ and $y = 0$ bins, which we do by taking $x \rightarrow 1$ and $y \rightarrow 0$. In this limit the gluon and b -quark in Fig. 2 become soft, and this region would be double counted without the zero-bin conditions. First consider the denominator,

$$\frac{1}{x + y - xy} = \frac{1}{(x + y)} + \frac{xy}{(x + y)^2} + \dots \quad (A2)$$

In the first term the x and y dependence does not decouple, so we must consider them simultaneously. All terms beyond the first one produce finite integrals and are dropped in the minimal subtraction scheme. For the numerator in Eq. (A1) we use $M_{pp}^{(1)}(0) = M^{(2)}(1) = 0$ and expand

$$\begin{aligned} M_{pp}^{(1)}(y) M^{(2)}(x) &= y_{pp}^{(0)}(0) x^{(0)}(1) - \frac{y^2}{2} \omega_{pp}^{(0)}(0) x^{(0)}(1) + y_{pp}^{(0)}(0) \frac{x^2}{2} \omega^{(0)}(1) + \dots \\ &= y_{pp}^{(0)}(0) \sum_{n=1}^{\infty} \frac{(-x)^n}{n!} \omega^{(n)}(1) - \frac{y^2}{2} \omega_{pp}^{(0)}(0) x^{(0)}(1) + \dots \end{aligned} \quad (A3)$$

In the first term on the last line we have identified all terms which remain singular when multiplied by $1/[xy^2(x + y)]$. This term is equal to $y_{pp}^{(0)}(0) (x)$. Taken together with the expansion of $x - y$ we therefore find that the required minimal subtraction is

$$\frac{y_{pp}^{(0)}(0) M^{(2)}(x)}{(x + y)xy^2} (x) - (y) : \quad (A4)$$

Following Ref. [18] we use this to convert Eq. (A 1) into an integral that includes the $x = 1$ and $y = 0$ regions,

$$\begin{aligned}
I &= \int_0^1 dx \int_0^1 dy \frac{M_{pp}^{M_1}(y) M_2(x)}{(x+y)xy^2} - \frac{y M_{pp}^{M_1 0}(0) M_2(x)}{(x+y)xy^2} \\
&\quad - \int_0^1 dx \int_0^1 dy \frac{y M_{pp}^{M_1 0}(0) M_2(x)}{(x+y)xy^2} x (1-x) y (y-1) + \int_0^1 dx \int_0^1 dy \frac{M_{pp}^{M_1 0}(0) M_2(x)}{(x+y)xy^2} y (y-1) \\
&= \int_0^1 dx \frac{M_2(x)}{x} \int_0^1 dy \frac{M_{pp}^{M_1}(y)}{(x+y)xy^2} - \frac{M_{pp}^{M_1 0}(0)}{(x+y)y} \int_0^1 dx \int_0^1 dy \frac{M_{pp}^{M_1 0}(0) M_2(x)}{(x+y)xy^2} y (y-1) \\
&= \int_0^1 dx \frac{M_2(x)}{x} \int_0^1 dy \frac{M_{pp}^{M_1}(y)}{(x+y)xy^2} - \frac{M_{pp}^{M_1 0}(0)}{(x+y)y} \int_0^1 dx \frac{M_2(x) \ln(2-x)}{(1-x)^2} :
\end{aligned} \tag{A 5}$$

Here in simplifying the term carrying the ultraviolet divergences as $y \rightarrow 1$, we noted that it is a powerlaw rather than logarithmic divergence, and so it does not induce dependence in our subtraction scheme. This result for I was used in Eq. (44). For the asymptotic pion wave functions, $\phi(x) = 6x(1-x)$ and $\phi_{pp}(y) = 6y(1-y)$, we obtain $I = 36 + 6^2 \cdot 144 \ln 2 = 4:60$. Note that the steps used here to derive the subtraction also give the correct result for cases where the x and y integrals factorize, such as an integrand $\phi(x) \phi(y) = (x^2 y^2)$.

-
- [1] C. W. Bauer, D. Pirjol and I. W. Stewart, Phys. Rev. Lett. 87, 201806 (2001) [hep-ph/0107002].
 - [2] M. Beneke, G. Buchalla, M. Neubert and C. T. Sachrajda, Phys. Rev. Lett. 83, 1914 (1999) [hep-ph/9905312]; M. Beneke, G. Buchalla, M. Neubert and C. T. Sachrajda, Nucl. Phys. B 591, 313 (2000) [hep-ph/0006124].
 - [3] S. Mantry, D. Pirjol and I. W. Stewart, Phys. Rev. D 68, 114009 (2003) [hep-ph/0306254].
 - [4] J. g. Chay and C. Kim, Phys. Rev. D 68, 071502 (2003) [hep-ph/0301055]; Nucl. Phys. B 680, 302 (2004) [hep-ph/0301262].
 - [5] C. W. Bauer, D. Pirjol, I. Z. Rothstein and I. W. Stewart, Phys. Rev. D 70, 054015 (2004) [hep-ph/0401188].
 - [6] C. W. Bauer, I. Z. Rothstein and I. W. Stewart, hep-ph/0510241.
 - [7] Y. Y. Keum, H. N. Li and A. I. Sanda, Phys. Lett. B 504, 6 (2001) [hep-ph/0004004];
 - [8] Y. Y. Keum, H. N. Li and A. I. Sanda, Phys. Rev. D 63, 054008 (2001) [hep-ph/0004173].
 - [9] C. D. Lu, K. Ukai and M. Z. Yang, Phys. Rev. D 63, 074009 (2001) [hep-ph/0004213].
 - [10] M. Beneke, G. Buchalla, M. Neubert and C. T. Sachrajda, Nucl. Phys. B 606, 245 (2001) [hep-ph/0104110].
 - [11] M. Beneke and M. Neubert, Nucl. Phys. B 675, 333 (2003) [hep-ph/0308039].
 - [12] M. Ciuchini, E. Franco, G. Martinelli and L. Silvestrini, Nucl. Phys. B 501, 271 (1997) [hep-ph/9703353]; M. Ciuchini et al., Phys. Lett. B 515, 33 (2001) [hep-ph/0104126].
 - [13] P. Colangelo, G. Nardulli, N. Paver and Riazuddin, Z. Phys. C 45, 575 (1990).
 - [14] H. n. Li, hep-ph/0408232.
 - [15] T. Feldmann and T. Hurth, JHEP 0411, 037 (2004) [hep-ph/0408188].

- [16] C.W.Bauer, S.Fleming and M.E.Luke, Phys.Rev.D 63, 014006 (2001) [hep-ph/0005275]; C.W.Bauer, S.Fleming, D.Pirjol and I.W.Stewart, Phys.Rev.D 63, 114020 (2001) [hep-ph/0011336]; C.W.Bauer and I.W.Stewart, Phys.Lett.B 516, 134 (2001) [hep-ph/0107001]; C.W.Bauer, D.Pirjol and I.W.Stewart, Phys.Rev.D 65, 054022 (2002) [hep-ph/0109045].
- [17] J.Mackles, hep-ph/0606083; Y.L.Wu and Y.F.Zhou, Phys.Rev.D 72, 034037 (2005) [hep-ph/0503077]; A.J.Buras, R.Fleischer, S.Recksiegel and F.Schwab, Nucl.Phys.B 697, 133 (2004) [hep-ph/0402112]; C.W.Chiang, M.Gronau, J.L.Rosner and D.A.Suprun, Phys.Rev.D 70, 034020 (2004) [hep-ph/0404073].
- [18] A.V.Mancher and I.W.Stewart, hep-ph/0605001.
- [19] M.A.Shifman, A.I.Vainshtein and V.I.Zakharov, Nucl.Phys.B 120, 316 (1977).
- [20] G.Buchalla, A.J.Buras and M.E.Lautenbacher, Rev.Mod.Phys. 68, 1125 (1996) [hep-ph/9512380].
- [21] A.J.Buras and L.Silvestrini, Nucl.Phys.B 569, 3 (2000) [hep-ph/9812392].
- [22] A.R.Williams and J.Zupan, hep-ph/0601214.
- [23] C.W.Bauer, S.Fleming, D.Pirjol, I.Z.Rothstein and I.W.Stewart, Phys.Rev.D 66, 014017 (2002) [hep-ph/0202088].
- [24] C.W.Bauer, D.Pirjol, I.Z.Rothstein and I.W.Stewart, Phys.Rev.D 72, 098502 (2005) [hep-ph/0502094].
- [25] M.Beneke, G.Buchalla, M.Neubert and C.T.Sachrajda, Phys.Rev.D 72, 098501 (2005) [hep-ph/0411171].
- [26] C.W.Bauer, D.Pirjol and I.W.Stewart, Phys.Rev.D 67, 071502 (2003) [hep-ph/0211069].
- [27] B.O.Lange and M.Neubert, Nucl.Phys.B 690, 249 (2004) [Erratum -ibid.B 723, 201 (2005)] [hep-ph/0311345].
- [28] H.n.Li, Czech. J. Phys. 53, 657 (2003) [Prog. Part. Nucl. Phys. 51, 85 (2003)] [hep-ph/0303116].
- [29] C.W.Bauer, D.Pirjol and I.W.Stewart, Phys.Rev.D 68, 034021 (2003) [hep-ph/0303156].
- [30] A.L.Kagan, Phys.Lett.B 601, 151 (2004) [hep-ph/0405134].
- [31] The Heavy Flavor Averaging Group (HFAG) (E.Barberio et al.), hep-ex/0603003, and updates at <http://www.slac.stanford.edu/xorg/hfag/>.
- [32] V.L.Chernyak and A.R.Zhitnitsky, Phys.Rept. 112, 173 (1984).
- [33] A.Hardmeier, E.Lunghi, D.Pirjol and D.Wyler, Nucl.Phys.B 682, 150 (2004) [hep-ph/0307171].
- [34] S.Wandzura and F.Wilczek, Phys.Lett.B 72, 195 (1977).
- [35] M.Beneke, A.P.Chapovsky, M.Diehl and T.Feldmann, Nucl.Phys.B 643, 431 (2002) [hep-ph/0206152].
- [36] M.Bander, D.Silverman and A.Soni, Phys.Rev.Lett. 43, 242 (1979).
- [37] T.Becher and R.J.Hill, JHEP 0410, 055 (2004) [hep-ph/0408344].
- [38] S.Mantry, D.Pirjol and I.W.Stewart, AIP Conf. Proc. 722, 141 (2004) [hep-ph/0401058]; D.Pirjol, hep-ph/0411124.
- [39] C.W.Bauer, I.Z.Rothstein and I.W.Stewart, Phys.Rev.Lett. 94, 231802 (2005) [hep-ph/0412120].
- [40] M.Beneke and S.Jager, hep-ph/0512351.
- [41] Y.Grossman, A.Hocker, Z.Ligeti and D.Pirjol, Phys.Rev.D 72, 094033 (2005) [hep-ph/0506228].
- [42] J.Charles et al. [CKM fitter Group], Eur.Phys.J.C 41, 1 (2005) [hep-ph/0406184].
- [43] A.Khodjamirian, T.Mannel, M.Melcher and B.Melic, Phys.Rev.D 72, 094012 (2005)

- [hep-ph/0509049].
- [44] A. Gray et al. [HPQCD Collaboration], Phys. Rev. Lett. 95, 212001 (2005) [hep-lat/0507015].
- [45] V. M. Braun et al., hep-lat/0606012.
- [46] P. Ball, V. M. Braun and A. Lenz, JHEP 0605, 004 (2006) [hep-ph/0603063].